Computer Communications 134 (2019) 163–184

Contents lists available at ScienceDirect

Computer Communications

journal homepage: www.elsevier.com/locate/comcom

A serious gaming approach to managing interference in ad hoc femtocell wireless networks

Abdullah Alhumaidi Alotaibi, Marios C. Angelides *

Department of Electronic and Computer Engineering, College of Engineering Design and Physical Sciences, Brunel University London, Uxbridge UB8 3PH, United Kingdom

A R T I C L E I N F O

Keywords:
Femtocell
Interference management
Optimisation

A B S T R A C T

The aim of this paper is to optimize femtocell performance by managing interference between femtocell devices and between a femtocell and a macrocell. It achieves this using a three-phase approach that involves deployment of femtocells and control of resulting connections through consideration and management of path loss, transmission power, signal strength and coverage area. Simulation experiments of the proposed three-phase approach at a local college that experiences a poor service from the macrocell predict significant improvements in femtocell performance in terms of managing both types of interference: co-tier and cross-tier, number of users who experience good service, coverage, and mitigating outage probability. The overall and individual complexity of each phase has also been considered. Our approach has been compared with some existing techniques chosen from the literature that has been reviewed and its predicted performance is significantly improved in comparison to these.

1. Introduction

Despite outperforming macrocells in indoor coverage, femtocell technology experiences significant levels of interference with other femtocells or a macrocell [1,2]. There are three broad types of schemes that are used to manage interference: Interference Cancellation, Interference Avoidance and Distributed Interference Management. Interference cancelation schemes focus on reducing interference at the receiver end and require knowledge of the interfering signal characteristics and antenna arrays at the receiver system to cancel any interference. These techniques are insufficient for user equipment but are suitable for implementation in base stations such as a macrocell Base Station (MBS) and Femtocell Access Point (FAP) and they produce good results when used for uplink interference management. Interference Avoidance schemes focus on adding intelligence to femtocell devices. Because of the ad hoc nature of femtocell deployment, it is difficult to manage femtocells from a centralized controller, therefore, intelligence is built into the FAP to enable it to self-organize and cope with interference. Providing the necessary knowledge to femtocells can be done through the backhaul network, but this would be one reason for causing congestion on it. Moreover, operators cannot provide information to femtocells through the backhaul, if their number is large. Distributed interference management enables femtocells to exchange information about their environment in order to manage interference. According to [3], femtocell deployment assumes a trade-off between spectrum availability and interference. Whereas in dedicated channels the spectrum is divided, in co-channels the spectrum is available to all users which may lead to higher cross-tier interference. A high transmission power causes interference to neighbouring FAPs and mobile base stations whereas a low transmission power limits the FAP coverage and in turn the service quality [4]. An adaptive transmission power is preferred over a fixed transmission power because in adaptive mode the transmission power can be altered by the FAP when necessary to avoid interference whereas it cannot in a fixed mode [5]. In [6] a path weight algorithm is suggested that estimates the available bandwidth. The algorithm aims at helping clients send packets through a best path which in return improves path throughput. In [7] a protocol entitled “Enhanced Receiver-Centric Interference” is deployed alongside an algorithm entitled “Nearest Component Connector” that yields a topology not affected by varying the number of nodes. In this research we consider the limitations of each of the three types of interference management schemes and propose a new technique that is a combination of three methods deployed as three phases. Firstly, a method which we call the deployment plan that identifies the best locations for deploying FAPs both indoors and outdoors. Secondly, a method which we call Find Best Node (FBN)

* Corresponding author.
E-mail addresses: abdullah.alotaibi@brunel.ac.uk (A.A. Alotaibi), marios.angelides@brunel.ac.uk (M.C. Angelides).

https://doi.org/10.1016/j.comcom.2018.07.013
Received 28 August 2017; Received in revised form 12 June 2018; Accepted 6 July 2018
Available online 13 November 2018
0140-3664/© 2019 The Authors. Published by Elsevier B.V. This is an open access article under the CC BY license (http://creativecommons.org/licenses/by/4.0/).

that finds the Best FAP (the Node) for each Femtocell User Equipment (FUE) among several candidate FAPs. FBN is executed by a Femtocell Management System (FMS) by considering several factors namely Received Signal Code Power (RSCP), multipath Path Loss (PL) and distance. Thirdly, a method which we call Best Node Keep Connected (BNKC) that enables a BN to maintain its level of service to its FUEs and thus reduce the probability of outage. BNKC is also executed by an FMS by managing the same parameters considered in FBN. The rest of this paper organized as follows: Section 2 reviews related work. Section 3 presents our research motivation, sourced from the review of related work. Section 4 discusses our three-phase approach for interference management. Section 5 presents a controlled experiment in interference management with our three-phase approach at a local college that experiences poor signal from the macrocell, followed by complexity analysis. Section 6 compares our approach to some existing techniques reported in the literature reviewed. Section 7 concludes.

2. Related works

Striking a balance between femtocell performance and interference has been widely researched. Some research practical solutions and as such they focus on managing interference issues, e.g. applying Supervised Mobile Assisted Range Tuning (SMART). SMART uses real measurements for transmission power calibration and it copes with all channel deployment scenarios and all femtocell access modes. This technique assumes technician assistance. Mobile feedback such as radio frequency, coverage range, and interference with other cells may be used to draft alternative deployments. SMART is suitable both as centralized and distributed [8] and may offer sufficient indoor femtocell. In [9] two algorithmic solutions to interference are suggested, namely, Finding Trouble Node (FTN) and Trouble Node Power Back-off (TAPB). These two methods identify the node that causes interference and then apply power control to decrease the interference. The results show that the approach of the proposed two methods is effective in enhancing the throughput of femtocell networks. In order to manage cross-tier interference, power control methods decrease the transmission power of a Home evolved Node B (HeNB). With these methods, the Macrocell evolved Node B (MeNB) and HeNB use all the bandwidth for interference management. Dynamic or adjustable power control can be performed either in Open Loop Power Setting (OLPS) or Closed-Loop Power Setting (CLPS) modes. An HeNB adjusts its transmission power proactively in the OLPS mode and reactively in the CLPS mode in coordination with MeNB. In a hybrid mode, HeNB alternates between the two. In [10] a distributed channel-aware power control scheme aims at creating spectrum reuse opportunities and coping with inter-femtocell downlink interference in OFDMA femtocell networks. Power control is presented as a Generalized Nash Equilibrium Problem (GNEP) and Variation Inequality (VI) theory is employed to address it. Numerical simulations show that there is significant capacity gain within a few iteration times. The proposed mechanism works by utilizing and merging potential spectrum reuse through downlink power control. In [11] a two-way pricing approach is applied into a Stackelberg game to prevent co-tier interference by controlling the uplink transmission. All Femtocell Base Stations (FBS) operate under the co-channel mode and use the same frequency band and operate in the Closed Subscriber Group (CSG) access mode. The leader FBS protects itself by pricing co-tier interference from follower FUEs to a maximum tolerable interference. In contrast, follower FUEs control transmission power based on the leader's pricing strategy. Simulation results show that leader and followers may achieve maximum utility on a Stackelberg Equilibrium (SE). In [12] a Mobile User Equipment (MUE) enhanced power control scheme measures the received power from its serving MBS and forwards the information to all surrounding FAPs. Path loss to each FAP is measured using Cognitive Radio (CR) to optimize power levels and prevent interference with the MUE. In [13] a centralised power control approach is proposed that uses cognitive radio sensing and power control and switches between access modes in order to identify white spaces or slots with low interference and self-configure. An SINR threshold is determined for each slot and a power control algorithm manages the transmission power to provide the required coverage. In [14] a centralised power control scheme uses Q-learning to allocate optimal power in order to manage cross-tier interference in the downlink. A FAP uses distributed learning to sense the radio environment, observe its state and obtain either a reward, i.e. low interference and high MUE capacity, or a penalty, i.e. high interference and low MUE capacity. Sensing over several rounds helps with evolving an optimal power allocation policy to manage interference and maintain MUE capacity. One drawback is a delay caused by the accumulated signalling overhead. In [15] a centralised power control scheme uses three phases, channel sensing, training and data transmission. During channel sensing, a FAP senses the radio environment to find an unoccupied spectrum, during channel training signals between the FAP and an FUE aimed at minimising the effect of path loss. [16] and [17] attempt to reduce path loss through estimation of the distances between nodes using real time RSSI. This approach minimises distance error and helps identify optimal locations for each node. In [18], two algorithms are applied: one to set transmission power and the other to adjust it. In [19], a Mobile Assisted Range Tuning (MART) technique exhibits superiority over the Network Listen Module alone technique due to its ability to maximise coverage. [20] and [21] prove that optimum coverage can be obtained by deploying small cells in appropriate locations based on a Poisson Point Process (PPP). This research suggests that FAPs should be installed close to each other in a macrocell coverage area and be considered as a second cluster. The research in [22] provides a solution to the issue of coverage by optimising the multi-femtocell deployment using genetics. The results show that it is possible to optimise multi-femtocell deployment without prior knowledge of the required number of FAPs. In [23] the authors consider modern buildings in their research as they practice severe penetration loss. Most deployment plans are not sufficient to solve this as outdoors deployments do not guarantee that the service provided to FUEs located inside buildings is sufficient. The research proves that indoor FAP deployment outperforms outdoors although it suffers high penetration loss. Their research suggest that deploying FAPs indoors in a co-channel approach achieves the best results. [24] considers femtocell deployment places, cell selection, and power control for optimisation. Their proposed solution increases user capacity after predicting the number of required femtocell devices within the macrocell coverage area. An algorithm, named "anytime algorithm" uses a coalition structure generation to provide the best deployment solution at specific times. Branch and Bound is used in [22] and [23] to optimise algorithms, as in [25] but with additional consideration of access mode and dedicated channel deployment. It is suggested that FAPs are deployed through a constant but dynamic frequency allocation plan that is suitable for a distributed 4 G femtocell network in order address the signalling overhead. In [26] the authors consider commercial buildings for FAP deployment and formulate a mathematical model as a Mixed Integer Convex Program (MICP) which is then applied using branch and bound. Their aim is to address mobile handset battery life and FAP deployment. Their results show that their technique provides an optimal solution to both issues. They predict accurately the best places to deploy FAPs inside a building. In [27] the research considers a three dimensional deployment for FAPs based on a propagation model prediction to resolve the two dimensional FAP deployment superiority with regards to both types of interference especially in an urban environment. In [28] a technique is applied in an LTE system where the path loss is shared among neighbouring FAPs. Not only path loss information is modified among FAPs but also information that belongs to the usage of LTE Component Carriers (CC). The information that relates to the CC is obtained using distributed carrier aggregation. FAPs exchange information using either an HeNB Femtocell Gateway (HeNB GW) or an Over-The-Air (OTA) method. The HeNB GW manages co-ordination information exchanges between FAPs and serves as intermediate node between FAPs and the mobile core

Table 1
Interference Management Techniques Advantages and Shortcomings.

Techniques	Spectrum access	Advantages	Shortcomings
Power control	Un-licensed [12], Licensed [9–11,42–44]	*Manages cross-tier, Increases throughput, Prevents leaking to outdoors, Improves capacity*	*Decreases coverage area, Poor SNR farthest to base station, Signalling overhead causes battery drain*
Spectrum arrangement	Un-licensed [45–54] Licensed [20,21,34–36,40,55–62]	*Addresses dead zone, Maximises Spectral efficiency, Improves capacity, Manages cross-tier interference*	*Introduces security concern, Prioritises MUE over FUEs, Complexity rises with number of FAPs*
Antenna	Un-licensed [63] Licensed [64–67]	*Single FUE target, nulls rest*	*Size-constrained FAP multi-antenna, Increased diversified-antenna costs*
Fractional Frequency *Re*-use	Licensed [32,68–77]	*Manages both types, Maximises network throughput*	*Difficult to implement in small areas*
Cognitive	Licensed [28]	*Manages "intelligently" co-tier*	*Manages "inefficiently" cross-tier*
Power calibration	Licensed [8,18,78–81]	*Good coverage, Reduces leakage to outdoors, Manages in large areas, Increases capacity*	*Manages "inefficiently" in small areas*
Joint schemes	Un-licensed, Licensed [33,37–39,41,82–84]	*Combines individual advantages*	*Introduces additional complexity, Raises signalling overhead*

network. The OTA connects FAPs and MBS by a direct link. The research presumes that each FAP can estimate co-tier interference based on path loss and that availability of CCs is accurately predicted. Each FAP can utilise a CC that is available for use: a CC that is not in use by other FAPs, a CC that is occupied by the furthest neighbour or a CC that is occupied by the least number of neighbours. The results illustrate that co-tier interference is minimised significantly. Table 1 collates much of the effort, including methods, perceived advantages and resulting issues. It lists six techniques alongside their spectrum accessibility since researchers report utilising both the licensed and unlicensed spectrum to exploit optimum solutions for interference. Some consider joint schemes to utilise collectively the advantages on offer from individual schemes. Some research utilises both the licensed and unlicensed spectrum for power control and spectrum arrangement. In [29] the authors present a simple way to predict the required number of FAPs and optimum place to locate them. They suggest that FAPs are located with consideration of macrocell interference and the level of SINR for each FAP. One of their aims is to predict the minimum number of FAPs for achieving coverage of their target building. They suggest that the distance between FAPs should be between a minimum value that is the root of three multiplied by half the FAP's coverage, and a maximum value that is equal to the FAP coverage distance where SINR is assured to be at the minimum level for all users. In [30] femtocell placement and power techniques are combined to enhance the power consumption and assure interference avoidance. The authors suggest that any area is divided into sub-regions equally, and then femtocells are placed appropriately at specific areas based on SNR values from the macrocell. Mixed integer programming is applied to ascertain optimum places for deployment and to minimise the required number of FAPs to prevent co-tier interference. Following that, the uplink transmission power is minimised using linear programming. The simulation results show that femtocells are deployed where the downlink and uplink interference is low. Moreover, energy consumption is enhanced. [31] propose a new method based on experimental measurements to provide users with optimum locations to receive high Quality of Service (QoS). This method is not only providing the best location to users but also predicting the movement path. Their suggested method, user-placement ushering mechanism, with which users are guided to their best places according to the accuracy of packet success rate PSR. Their method is presented in two phases. Firstly, during an offline phase indoor geographical QoS is mapped either based on experimental measurements or an interference model that is used to convert the SINRs at the physical layer into the PSRs at the MAC layer. QoS could be mapped geographically by measuring the area and exploiting both network topology and path loss model. Secondly, during an online phase the mapped PSR is used to predict the closest optimum location to offer high QoS for such a user. A femtocell can serve its user with the best close location after receiving the current location for its users through indoor position techniques. Femtocell is informed by the QoS requirements so a new place is suggested if the PSR is less than the required level. Femtocells provide their users with suggested places via the downlink control channel. One shortcoming with this method is an error in the accuracy while predicting the QoS requirements. In [32] researchers propose a technique based on group reuse spectrum auction mechanism for FFR (GRSAF). A group buying is applied to utilise the auction process and share the spectrum optimally. Their technique suggests that each buyer group who use the same spectrum is considered as a virtual group who joins the competition of spectrum auction. The auction strategy is presented in four steps. Firstly, secondary users always try to increase their benefits. Secondly, buyers will pay no less than their true bids. Thirdly, there should be a balance between the amount paid and reward received for buyers, i.e. buyers should receive the value they deserve. Finally, the efficiency is presented as the difference between what is paid and received between sellers and buyers. The high efficiency is provided to the buyers who pay more in comparison to others. Results show that spectrum is utilised optimally and the sum utility is enhanced. Moreover, the co-channel interference is addressed. In [33], it is suggested that interference among femtocell devices could be mitigated by dividing the spectrum among them. The proposed technique combines indoor deployment and cluster-based resource allocation and it takes into account three factors: identifying the optimal location at which to install the FAPs which form the cluster, selecting the cluster head based on a number of neighbour FAPs, and the number of the users to assign the required portion of the available spectrum. The results show that both coverage and capacity are maximised and both outage probability and co-tier interference are totally mitigated. Resource allocation has recently been considered for addressing interference in [34–37] using either game theory or optimisation techniques. In [38] a new technique is presented which considers hybrid access mode for users, reduces interference and maximises system performance. This technique relies on channel allocation and power control. It utilises game theory to address priority-based access which requires distinction between primary and secondary users. It assumes that each FAP is connected to the users at specific transmission power value subject to user priorities. In hybrid access mode, users subscribing to FAPs services have the choice of connecting either to the FAPs or the nearby macrocell, whereas non-subscribers can only connect to the macrocell. However, the authors argue that subscribers should only have access to FAPs, when this is available, and be blocked from connecting to the macrocell. Furthermore, they argue that non-subscribers should also have the same choice as subscribers have in order to achieve the highest possible quality of service. Their results suggest that network capacity is increased, interference is minimised and the probability of outage is reduced. The authors argue that their technique outperforms all other access modes techniques especially in relation to increasing total revenue for the service provider whilst ensuring reasonable prices for users. Hybrid access mode is also considered in [39] where the authors address delay by deploying a greedy algorithm to lexicographic admission control on the incoming traffic data flows. Moreover, they argue that the problem of non-convex maximization could be addressed

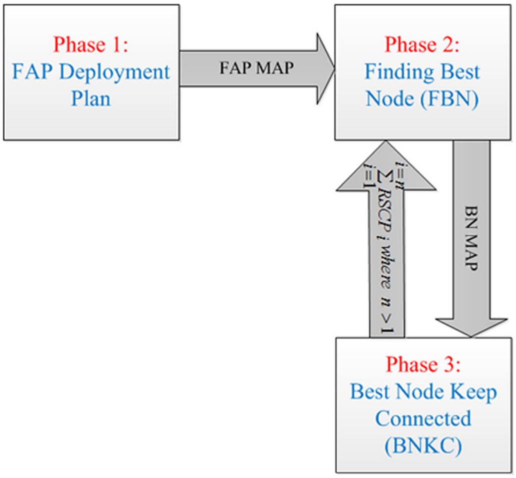

Fig. 1. Three phase interference management.

by using a suboptimal delay-bound packet scheduling and dual decomposition power allocation algorithm. The authors argue that as a result of bounded packet delays and power constraints, the weighted sum rate of each femtocell is increased. Their predictions demonstrate the superiority of their proposed scheme over other schemes in relation to the quality of service level that may be achieved. The authors also argue that their scheme also achieves high throughput and fairness. In [40] it is reported that interference is addressed by allocating subchannels to each user. A user-centric coalition formation game helps with identifying those users who interfere with other users and graph theory helps with assigning these users to available subchannels. Likewise in [41], cochannel interference is addressed by allocating subchannels to each user. A non-cooperative game helps with assigning subchannel to each user while keeping transmission power as low as possible.

3. Research motivation

The primary research motivation is to address interference, i.e. co-tier between FAPs or cross-tier between FAPs and a macrocell. Secondary research motivations include addressing of femtocell coverage, or shortage of, especially indoors which may lead to a decrease in service quality, and of outage probability often caused by *ad hoc* FAP deployment. Power calibration techniques, such as SMART, yield good coverage, reduction of leakage outside a building, interference management in large area, and increase in capacity. However, the same issues these techniques attempt to address often evolve as their drawbacks, i.e. leakage due to high multipath, extent of coverage not accurately predicted until after full FAP deployment which if *ad hoc* will raise both the probability of outage and coverage gaps. Varying the transmission power and not keeping it constant helps with managing co-tier and importantly cross-tier interference. Likewise, cognitive approaches aim at managing co-tier interference intelligently which in turn will improve throughput. However, as the number of FAPs grows their success with co-tier management drops since they depend heavily on occupying the unused carrier and thus reducing the spectral efficiency. Power control aims at minimising cross-tier interference which in turn will increase throughput. However, minimising transmission power in their attempt to manage cross-tier, results in coverage shrinks. These techniques yield poor SNR as users move further away from the base station and signal overheads that may occur as a result will cause battery drain. In our research we aim to address the drawbacks presented above with interference management being at the forefront of our work commencing with predicting the required number of FAPs to achieve full coverage, developing a deployment plan that considers RSCP, PL and distance to identify the next FAP location but varying the transmission power between a lower and an upper level to both manage any interference and address potential outage.

4. Three-phase gaming approach to interference management

Our proposed interference management method comprises of three main algorithms that are deployed over three phases. The first algorithm is a deployment plan technique which calibrates initial transmission power for femtocell devices before and immediately after deployment. This technique relies on power calibration to identify the best location for installing the next FAP. It accommodates both indoor and outdoor deployment. The second algorithm, FBN, identifies the best FAP for each FUE using the Auction and Stackelberg game algorithms. The third algorithm, BNKC, allows a FAP that connects to an FUE to increase its transmission power if there is an absence of other nodes and the FUE moves to a location that receives no signal. FMS is used to organise and compare information received from each device in order to disconnect and connect FUEs to FAPs. FMS plays an important role in minimising interference and, hence, improving the performance of femtocell technology. Fig. 1 shows all three algorithms over the three phases.

Phase 1: FAP Deployment Plan

This phase is carried out in two steps. The first step is an indoor deployment plan. The second step is an outdoor deployment plan. However, before these two steps two different experiments need to be carried out; firstly, a femtocell device is installed inside an anechoic chamber to solicit its properties especially its transmission power; secondly, the femtocell device is deployed indoor to estimate path loss and penetration loss. FAPs are connected to their respective operator networks and then have their transmission power boosted to achieve their maximum coverage of approximately 50 m. A FAP is capable of simultaneous connection with 16 FEUs in closed access mode. The number of FAPs necessary to achieve the optimum coverage needs to be estimated:

$$\mathbf{NoFAPs} = \frac{(\mathbf{L} \times \mathbf{W})}{\boldsymbol{D'}^2} \quad (1)$$

where NoFAPs is the number of FAPs required, L and W denote length and width of the target area and D` is the threshold radius.

Step 1: Indoor deployment plan

The locations chosen to install FAPs depend on RSCP values. Calibration is similar to the SMART method as it assumes technician supervision in identifying places of deployment for the first FAP. Table 2 shows the range of measurements taken, i.e. D, RSCP, multipath value (PI) and Transmission Power (Pt) which is fixed at 10 dBm until completion of deployment. Thereafter, the transmission power is controlled to avoid interference and the probability of outage. These measurements are necessary in identifying the best location of the next FAP.

Experiments in an anechoic chamber show the weakest signal is received at 45°. Starting at the centre (c) of the target coverage area testing is carried out in 5 m intervals in a 45° direction:

$$\boldsymbol{T_c} \rightarrow [\boldsymbol{L}/2, \boldsymbol{W}/2]$$

$$\textbf{For all } \mathbf{T_1} \ldots \mathbf{T_N} \textbf{ where } \mathbf{N} >= 1$$

$$\boldsymbol{T_N} \rightarrow \theta + (\theta \times (\boldsymbol{N} - 1))\, \boldsymbol{T_c} @\ 5\boldsymbol{m} \quad (2)$$

where T_c is the test carried out in the centre of the target area, → points to the 2D direction of a test, L is the length of a building, W is the width

Table 2
Range of measurements taken.

D	RSCP	Pl	Pt
@ 5 m intervals	dBm	dBm	10 dBm

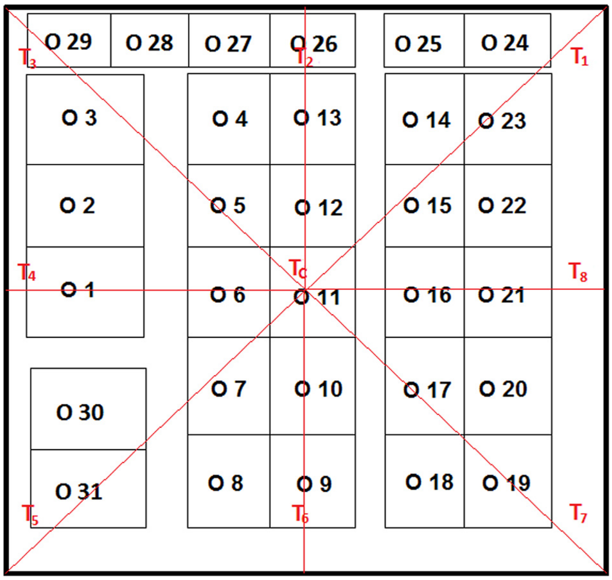

Fig. 2. Initial testing.

of a building, [L/2, W/2] denotes the centre of the building, T_N denotes each test carried out, θ is the 45° testing angle, and $(\theta \times (N-1))\, T_c @ 5m$ refers to the 2D direction of each test carried out at 5 m intervals from the centre (c). Fig. 2 shows an example of this initial testing.

Once testing has identified a location where there is either no signal from the macrocell or the RSCP from the macrocell is at its weakest, the first FAP is installed. Further testing to identify subsequent locations is carried out:

For all $T_1 \ldots T_N$ where N >= 1

$$T_N \rightarrow \theta + (\theta \times (N-1))\, FAP_{N-1} @ 5m \tag{3}$$

where T_N denotes each test carried out, FAP_{N-1} refers to last FAP installed, and $(\theta \times (N-1))\, FAP_{N-1} @ 5\ m$ refers to the 2D direction of each test carried out at 5 m intervals from last FAP installed. Fig. 3 shows testing post-installation of first FAP.

We further demonstrate our approach in the case where the NoFAPs calculation returns 3 FAPs. FAP_1 is installed at a location where there either is no signal received from the macrocell or the RSCP from the macrocell is at its weakest. After deployment of FAP_1, FAP coverage and the outage probability are estimated again. RSCP is measured at 5 m intervals in 45° directions from FAP_1 to locate the weakest received signal. This operation is repeated after deployment of each subsequent FAP. FAP_2 is installed where the RSCP from the FAP_1 is at its weakest

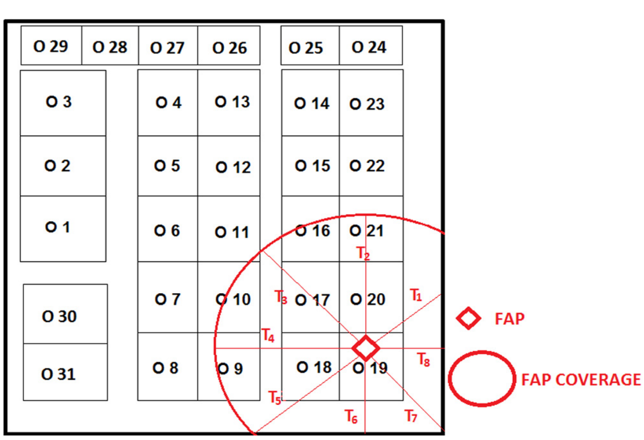

Fig. 3. Testing post-installation of first FAP.

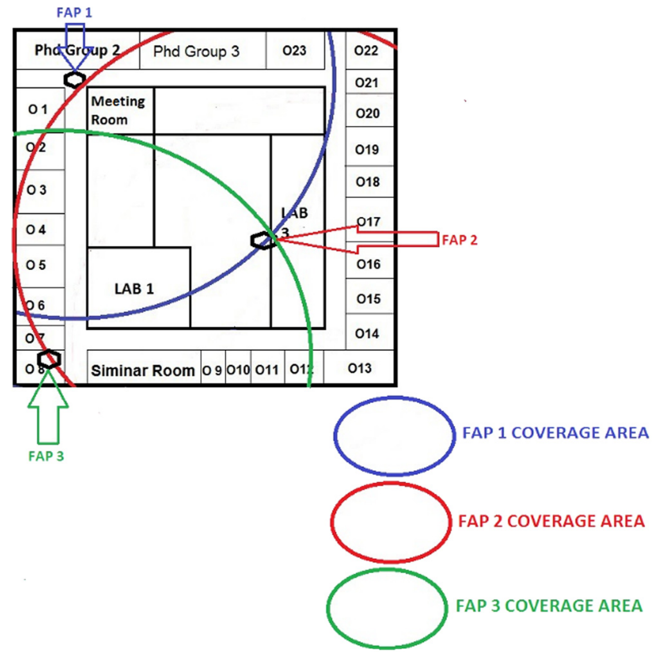

Fig. 4. Example of deployment of 3 FAPS.

and FAP_3 is installed where the RSCP from FAP_2 is at their weakest, and henceforth, in cases where the formula has returned more than 3 FAPs as being necessary. In the case of installing FAP_1, if the weakest macrocell RSCP value is reported in more than one location, then FAP_1 is deployed where it provides optimal coverage. In the case of FAP_2, if the weakest FAP RSCP value is reported at two locations, FAP_2 is deployed where it may provide optimal coverage otherwise installed at a 45° from FAP_1. FAP_3 and any FAPs thereafter are installed accordingly. Fig. 4 gives an example of how the three FAPs may be deployed.

Transmission power is initially set at a lower level than the maximum transmission power 20 dBm which is enough to cover the target area. The purpose of setting the transmission power at such a low level is to utilise as much of the remaining power to overcome any outage. Moreover, reducing transmission power helps with minimising cross-tier interference. Therefore, FAP_1 deployment continues as:

$$FAP_1 = \begin{cases} Min\,\{RSCP_{macro}\} \\ Max\,\{coverage\} \end{cases} \tag{4}$$

whereas deployment of the remaining FAPs continues as:

For all $FAP_2 \ldots FAP_n$ where $n >= 2$

$$FAP_n = \begin{cases} Min\,\{RSCP_{n-1}\} \\ Max\,\{coverage\} \\ \theta = 45^\circ \end{cases} \tag{5}$$

FAP_1 refers to the first deployed FAP, $Min\,\{RSCP_{macro}\}$ refers to the lowest RSCP from the macro base station, FAP_n denotes the next FAP to be deployed, $Min\,\{RSCP_{n-1}\}$ refers to the minimum RSCP received from a FAP and θ refers to 45° angle from the last FAP that has been deployed.

Step 2: Outdoor deployment Plan

For an outdoor environment testing in a 45° direction at regular intervals does not work well; results from several experiments leave a significant amount without coverage. Instead, to predict more accurately the probability of outage, the target area is scanned both

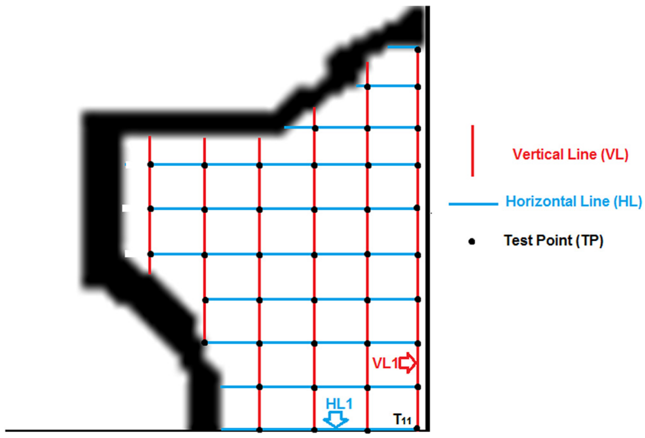

Fig. 5. Initial test plan for outdoors.

vertically, either top to bottom or vice versa, and horizontally, either left to right or vice versa, starting with the longest stretch. Testing is carried out at the intersection of each horizontal and vertical line. The distance between adjacent vertical or horizontal lines should not exceed half the distance threshold to prevent any potential co-tier interference, if testing results in two FAP_S being necessary. After deploying the first FAPs, unlike indoor deployment more than one FAP may initially be necessary for outdoors, the test to install other FAPs continues as with the indoor test. Testing outdoors for installation of the first FAPs is carried out as:

$$\sum\nolimits_m^n \boldsymbol{T}_{mn} = \boldsymbol{HL}_m \cap \boldsymbol{VL}_n @ \boldsymbol{D}$$
$$\textbf{where } \boldsymbol{m} = 1 \ldots \boldsymbol{m} \ \textbf{ and } \ \boldsymbol{n} = 1 \ldots \boldsymbol{n}$$
$$\textbf{where } \ \boldsymbol{D} = \boldsymbol{D}' \times 2 \ \textbf{between } \ \boldsymbol{VLs} \ \textbf{ and } \ \boldsymbol{HLs} \tag{6}$$

where T_{mn} are tests carried out at intersections, m = number of horizontal lines, n = number of vertical lines, and D is the distance either between vertical VLs or horizontal lines HLs. Fig. 5 depicts initial testing at T_{11} outdoors which sits on the longest stretch. Fig. 6 shows initial outdoor deployment of FAPs. Outage may still be experienced following deployment, for example, the area between FAP_1 and FAP_2. However, outage is managed as each FAP's RSCP is re-tested and deployment continues. Figs. 7 and 8 depict further deployment.

Phase 2: Finding Best Node (FBN)

The FBN algorithm considers the RSCP, PL and D between FAPs and FUEs to find the BN, i.e. FAP, for each FUE located within an interference area. All other FAPs within the interference area are considered as the source of the interference, aptly called TANs (To Avoid Nodes).

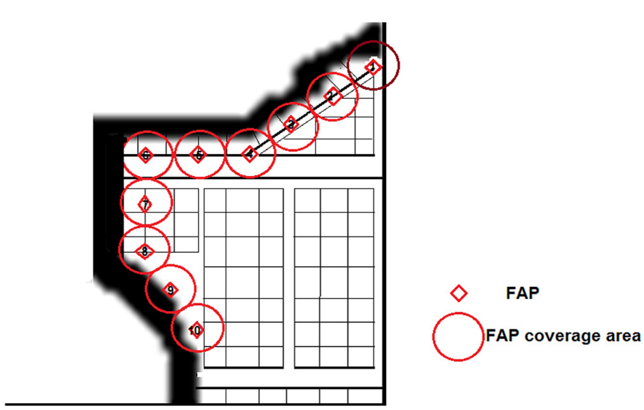

Fig. 6. Initial outdoor deployment.

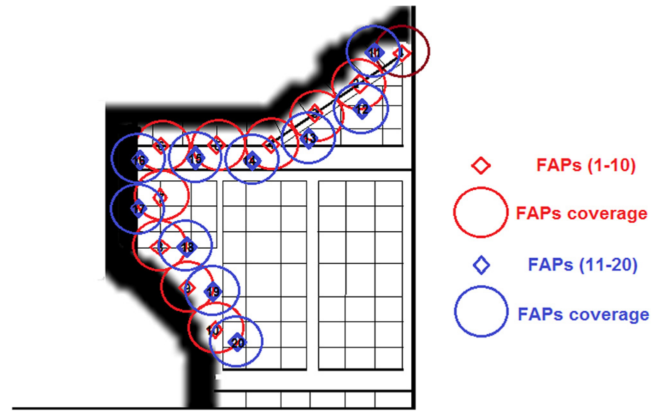

Fig. 7. Post-initial outdoor deployment.

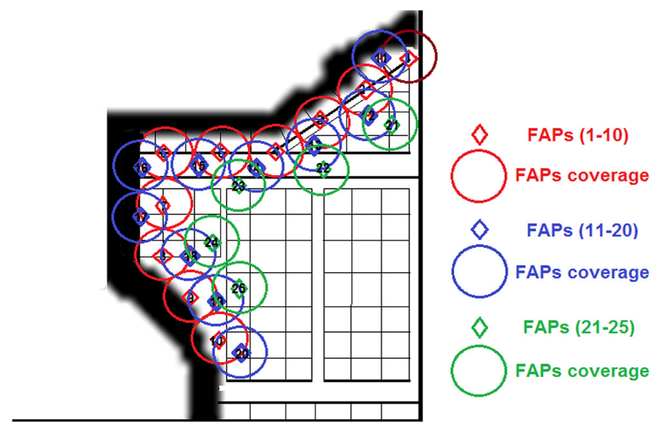

Fig. 8. Further outdoor deployment.

RSCP and PL are measured by a mobile application whereas D is either measured manually or predicted. The FMS controls the connections between FAPs and FUEs. There are two main conditions to connecting each FUE to a FAP: first, it must be within a FAP radio threshold, and second, it must not receive an RSCP that is less than the highest $RSCP_{macro}$. With respect to PL, using the Extended Dual Slope (EDS) path loss model [85], the loss at specific locations in a building is:

$$\boldsymbol{PL} = \boldsymbol{PL}_r + \boldsymbol{k} \times \mathbf{10log_{10}} \left(\frac{\boldsymbol{d}}{\boldsymbol{r}}\right) + \sum_{\boldsymbol{w}}^{\boldsymbol{n}} \left(\boldsymbol{Lw}^* \boldsymbol{n} + \boldsymbol{Hw}^* \boldsymbol{n}\right) \tag{7}$$

where PL_r is the path loss at a reference point r, K is the path loss exponent, d denotes distance, R is distance between a reference point and a FAP, Lw and Hw are light and heavy walls respectively, n denotes number of walls. ***RSCP*** is calculated as:

$$\boldsymbol{RSCP} = \boldsymbol{P}_t - \boldsymbol{PL} \tag{8}$$

The FBN algorithm uses a hybrid game approach to determine the best node: auction game theory with Stackelberg competition. We use the first price auction concept whereby the highest bidder wins the payoff:

$$\boldsymbol{b}_i^* = \boldsymbol{max} \ \{\boldsymbol{b}_i\} \tag{9}$$

where b_i^* is the highest bid and b_i denotes a bid provided by any bidder. In the case of two bidders the strategies and payoffs are:

$$\boldsymbol{u}_i(\boldsymbol{b}_1) = \begin{cases} \boldsymbol{b}_i^* & \boldsymbol{if} \ \ \boldsymbol{b}_i > \boldsymbol{b}_j \\ \frac{\boldsymbol{b}_i^*}{2} & \boldsymbol{if} \ \ \boldsymbol{b}_i = \boldsymbol{b}_j \\ \mathbf{0} & \boldsymbol{if} \ \ \boldsymbol{b}_i < \boldsymbol{b}_j \end{cases} \tag{10}$$

where u_i (b_1) denotes the payoff of the first bidder, b_i denotes the bid of first bidder and b_j refers to the bid of the second bidder. The equation denotes that if the first bidder offers the highest bid, the first bidder wins the payoff whereas if the first bidder offers the lowest, the first bidder loses the payoff. If both bidders make an equal bid, the winner is usually chosen by a coin toss in auction theory but this option is resolved through Stackelberg competition in our approach as bidding comprise of separate values from three separate parameters thus payoff may not be decided by the first parameter value but subsequent values.

The three parameters comprise the bid, the FAPS represent the players and the payoff is BN to the FUE requesting connection. The FAP strategy, managed by the FMS, involves satisfying the following conditions:

1. Its RSCP is higher than the RSCP threshold RSCP′
2. Its distance to the FUE is less than the distance threshold D′

Hence,

$$\textit{If}\ \ \boldsymbol{FAP}_{i_{RSCP}} > \boldsymbol{RSCP'}\ \textit{and}\ \boldsymbol{FAP}_{i_D} < \boldsymbol{D'}$$
$$\textit{THEN}\ \boldsymbol{FAP}_i \approx \boldsymbol{BN}$$

Any FAPs satisfying these conditions may compete to provide connection to an FUE using the auction game approach. If there are more than one FAPs competing, the BN chosen is that which satisfies one of these conditions in comparison to other FAPs:

1. Its RSCP is the highest

   $\boldsymbol{Max}\,\{\boldsymbol{RSCP}_i\}$

2. Its multipath is the lowest

   $\boldsymbol{Min}\,\{\boldsymbol{PL}_i\}$

3. Its distance to the FUE is the shortest

   $\boldsymbol{Min}\,\{\boldsymbol{D}_i\}$

In the case where the RSCP values of several FAPs are the same, the multipath and distance values are considered in selecting the BN. Hence, our auction game payoff function for FAP_i starts as:

$$\boldsymbol{BN}^{RSCP_i}_{FUE_j} = \begin{cases} \boldsymbol{Max}\,\{\boldsymbol{RSCP}_i\} \\ \boldsymbol{PL}^*_i \\ \varnothing \end{cases} \tag{11}$$

where $\boldsymbol{Max}\,\{\boldsymbol{RSCP}_i\}$ denotes highest price and designates FAP_i as BN, $\boldsymbol{PL}^*_i$ checks the multipath value if RSCP values are all equal, $\varnothing$ denotes disconnection of FUE_j to a FAP if it does not offer the highest RSCP. In the case where two or more optimum RSCPs are reported consideration shifts to PL:

$$\boldsymbol{BN}^{PL_i}_{FUE_j} = \begin{cases} \boldsymbol{Min}\,\{\boldsymbol{PL}_i\} \\ \boldsymbol{D}^*_i \\ \varnothing \end{cases} \tag{12}$$

where $\boldsymbol{Min}\,\{\boldsymbol{PL}_i\}$ denotes lowest price and designates FAP_i as BN, $\boldsymbol{D}^*_i$ checks the distance to a FAP from an FUE in the case where two or more minima PLs are reported:

$$\boldsymbol{BN}^{D_i}_{FUE_j} = \begin{cases} \boldsymbol{Min}\,\{\boldsymbol{D}_i\} \\ \boldsymbol{Stac}^* \\ \varnothing \end{cases} \tag{13}$$

where $\boldsymbol{Min}\,\{\boldsymbol{D}_i\}$ denotes the lowest distance between an FUE and FAP_i, $\boldsymbol{Stac}^*$ is the Stackelberg value (instead of choosing at random) when all distance values are equal. Hence, the BN for each FUE is as follows with Stackelberg applied if there is more than one best node:

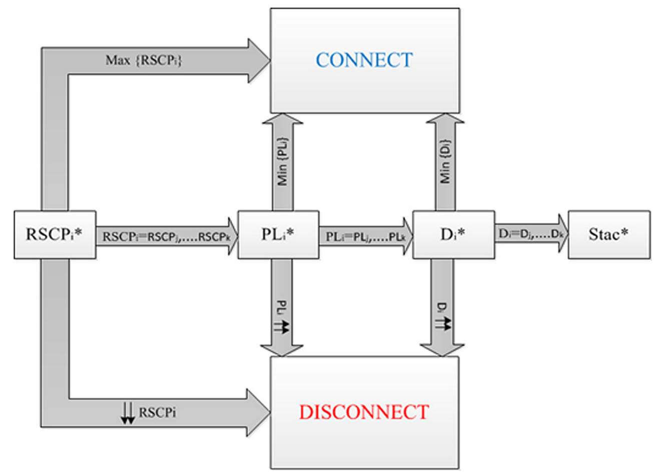

Fig. 9. The BN equation as a decision diagram.

$$\boldsymbol{BN}_{FUE_j} = \begin{cases} \boldsymbol{Max}\,\{\boldsymbol{RSCP}_i\} \\ \begin{cases} \boldsymbol{Min}\,\{\boldsymbol{PL}_i\} \\ \begin{cases} \boldsymbol{Min}\,\{\boldsymbol{D}_i\} \\ \boldsymbol{Stac}^* \\ \varnothing \end{cases} \\ \varnothing \end{cases} \\ \varnothing \end{cases} \tag{14}$$

Fig. 9 We use Stackelberg competition to avoid having to make a random choice when the values of all parameters are the same for the candidate FAPs. Whilst it is unlikely to identify two or more candidate FAPs with the same values, Stackelberg competition may be used as part of our approach in managing interference that is likely to arise. Stackelberg competition between two firms, in our case between two FAPs, is:

$$\boldsymbol{P} = \boldsymbol{a} - \boldsymbol{b} \times \boldsymbol{Q}_i \tag{15}$$

where $\boldsymbol{P}$ is the curve demand of power, $\boldsymbol{a}, \boldsymbol{b}$ are constant weights which can be set to specific values in consideration of quantity, $\boldsymbol{Q}_i$. In the case of two firms, $\boldsymbol{Q}_i$ is the sum of their respective quantities $\boldsymbol{Q}_1$ and $\boldsymbol{Q}_2$:

$$\boldsymbol{R}_1 = \boldsymbol{P} \times \boldsymbol{Q}_1 = (\boldsymbol{a} - \boldsymbol{b} \times \boldsymbol{Q}_1) \times \boldsymbol{Q}_1 = \boldsymbol{aQ}_1 - \boldsymbol{bQ}_1^2$$

$$\boldsymbol{MR}_1 = \lim_{\boldsymbol{Pt}_{min} \to \boldsymbol{Pt}_{max}} \frac{\partial \boldsymbol{R}_1}{\partial \boldsymbol{Q}_1} \to \boldsymbol{MR}_1 = \boldsymbol{a} - 2\boldsymbol{bQ}_1$$

$$\boldsymbol{MR}_1 = \boldsymbol{MC}_1 = 0 \to \boldsymbol{Q}_1 = \frac{\boldsymbol{a}}{2\boldsymbol{b}}$$

$$\boldsymbol{R}_2 = \boldsymbol{P} \times \boldsymbol{Q}_2 = \left(\boldsymbol{a} - \boldsymbol{b} \times (\boldsymbol{Q}_1 + \boldsymbol{Q}_2)\right) \times \boldsymbol{Q}_2 = \left(\boldsymbol{a} - \boldsymbol{b} \times \boldsymbol{Q}_1 - \boldsymbol{b} \times \boldsymbol{Q}_2\right) \times \boldsymbol{Q}_2$$
$$= \left(\boldsymbol{aQ}_2 - \boldsymbol{bQ}_1\boldsymbol{Q}_2 - \boldsymbol{bQ}_2^2\right)$$

$$\boldsymbol{MR}_2 = \lim_{\boldsymbol{Pt}_{min} \to \boldsymbol{Pt}_{max}} \frac{\partial \boldsymbol{R}_2}{\partial \boldsymbol{Q}_2} \to \boldsymbol{MR}_2 = \boldsymbol{a} - \boldsymbol{bQ}_1 - 2\boldsymbol{bQ}_2$$

$$\boldsymbol{MR}_2 = \boldsymbol{a} - \boldsymbol{b}\frac{\boldsymbol{a}}{2\boldsymbol{b}} - 2\boldsymbol{bQ}_2 = \frac{\boldsymbol{a}}{2} - 2\boldsymbol{bQ}_2$$

$$\boldsymbol{MR}_2 = \boldsymbol{MC}_2 = 0 \to \boldsymbol{Q}_2 = \frac{\boldsymbol{a}}{4\boldsymbol{b}} = \frac{\boldsymbol{Q}_1}{2}$$

where R_1 and R_2 denote respective peak minimum transmission Power (TP) values, MR_1 and MR_2 denote respective variations in peak minimum transmission Power values (MTP) which is set at 0. In addition, $\boldsymbol{Pt}_{max}$ is the peak maximum transmission power set at 20 dBm, $\boldsymbol{Pt}_{min}$ is the initial transmission power set at 10 dBm and MC_1 and MC_2 are respective variations in initial transmission power Pt (MPt) which is set at 0. The first mover is the first installed thus its power is maximised twice as much in comparison to the second FAP.

Stackelberg competition is deployed to avoid having to make a random choice during auction thus enabling candidate FAPs to compete against each other for providing connectivity to the target FUE. Stackelberg presumes that the target FUE located at the same distance from the competing FAPs, their multipath values to it are equal, and that the FUE experiences equal levels of power from the competing FAPs. We consider transmission power as the Stackelberg quantity and marginal cost is assumed to be 0. Constant a is set at 20 dBm to equal the maximum transmission power, $a = Pt_{max}$, and constant b is set at the value of the ratio between the initial transmission power of 10 dBm and the maximum of 20 dBm, $b = \frac{Pt_{min}}{Pt_{nax}} = 0.5$ dB

$$\boldsymbol{P = a - bQ_i = 20 - 0.5\left(Pt_{FAP_i}\right)} \tag{16}$$

In the case where there are three FAPs competing for BN:

$$\boldsymbol{P = Pt_{max} - \frac{Pt_{min}}{Pt_{max}}\left(Pt_{FAP_1} + Pt_{FAP_2} + Pt_{FAP_3}\right)}$$

$$\boldsymbol{P_1 = Pt_{max} - \frac{Pt_{min}}{Pt_{max}}\left(Pt_{FAP_1}\right)}$$

$$\boldsymbol{TP_1 = P_1 \times \left(Pt_{FAP_1}\right)}$$

$$\boldsymbol{TP_1 = \left(Pt_{max} - \frac{Pt_{min}}{Pt_{max}}\left(Pt_{FAP_1}\right)\right) \times \left(Pt_{FAP_1}\right)}$$

$$\boldsymbol{MTP_1 = \lim_{10\to 20}\frac{\partial TP_1}{\partial Pt_{FAP_1}} = Pt_{max} - 2\frac{Pt_{min}}{Pt_{max}}(Pt_{FAP_1})}$$

$$\boldsymbol{MTP_1 = MPt_1} = 0 \rightarrow \boldsymbol{Pt_{FAP_1} = \frac{20}{2\times 0.5} = 20\ dB}$$

With Stackelberg competition Pt_{FAP_1} is set to the maximum transmission power:

$$\boldsymbol{P_2 = Pt_{max} - \frac{Pt_{min}}{Pt_{max}}\left(Pt_{FAP_1} + Pt_{FAP_2}\right)}$$

$$\boldsymbol{TP_2 = P_2 \times \left(Pt_{FAP_2}\right)}$$

$$\boldsymbol{= \left(Pt_{max} - \frac{Pt_{min}}{Pt_{max}}\left(Pt_{FAP_1}\right) - \frac{Pt_{min}}{Pt_{max}}\left(Pt_{FAP_2}\right)\right) \times \left(Pt_{FAP_2}\right)}$$

$$\boldsymbol{MTP_2 = \lim_{10\to 20}\frac{\partial TP_2}{\partial Pt_{FAP_2}} \rightarrow = Pt_{max} - 4\frac{Pt_{min}}{Pt_{max}}\left(Pt_{FAP_2}\right)}$$

$$\boldsymbol{MTP_2 = MPt_2} = 0 \rightarrow \boldsymbol{Pt_{FAP_2} = \frac{20}{4\times 0.5} = 10\ dB}$$

With Stackelberg competition $Pt_{FAP_2} = \frac{max\{Pt\}}{2} = \frac{Pt_{FAP_1}}{2}$

$$\boldsymbol{P_3 = Pt_{max} - \frac{Pt_{min}}{Pt_{max}}\left(Pt_{FAP_1} + Pt_{FAP_2} + Pt_{FAP_3}\right)}$$

$$\boldsymbol{TP_3 = P_3 \times (Pt_{FAP_3})}$$

$$\boldsymbol{= \left(Pt_{\max} - \frac{Pt_{\min}}{Pt_{\max}}(Pt_{FAP_1}) - \frac{Pt_{\min}}{Pt_{\max}}(Pt_{FAP_2}) - \frac{Pt_{\min}}{Pt_{\max}}(Pt_{FAP_3})\right) \times (Pt_{FAP_3})}$$

$$\boldsymbol{MTP_3 = \lim_{10\to 20}\frac{\partial TP_3}{\partial Pt_{FAP_3}} \rightarrow = Pt_{max} - 8\frac{Pt_{min}}{Pt_{max}}\left(Pt_{FAP_3}\right)}$$

$$\boldsymbol{MTP_3 = MPt_3 = 0 \rightarrow Pt_{FAP_3} = \frac{20}{8\times 0.5} = 5\ dB}$$

With Stackelberg competition $Pt_{FAP_3} = \frac{max\{Pt\}}{4} = \frac{Pt_{FAP_2}}{2}$. Minimum transmission power should not be less than the initial transmission power $Pt_{FAP_3} = 10$ dB.

Phase 3: Best Node Keep Connected (BNKC)

If there is no received signal from another FAP or the macrocell FUEs remain connected to the FAP which has been designated their BN, regardless of the threshold distance, D`. BN transmission power may be controlled, if necessary, to enable a BN to maintain its level of service to its FUEs. An FUE may be kept connected to its BN either without any change to the BN transmission power or by having to increase it. A BN's transmission power is not changed when the $\boldsymbol{RSCP_{BN}}$ is higher than the $\boldsymbol{RSCP'}$ as the signal is sufficient to maintain a connection to the FUE without causing any interference. In this case, BN transmission power $\boldsymbol{Pt'_{BN}}$ is set to $\boldsymbol{Pt_{min}}$:

$$\boldsymbol{Pt'_{BN} = Pt_{min}\quad iff\quad RSCP_{BN} \geq RSCP'} \tag{17}$$

A BN's transmission power may be increased if the $\boldsymbol{RSCP_{BN}}$ is less than the $\boldsymbol{RSCP'}$ and their difference is higher than $\boldsymbol{Pt_{min}}$ but less than $\boldsymbol{Pt_{max}}$. In this case, the BN transmission power $\boldsymbol{Pt'_{BN}}$ is set to their difference value:

$$\boldsymbol{Pt'_{BN} = RSCP' - RSCP_{BN}} \tag{18}$$

$$\boldsymbol{iff\quad Pt_{min} \leq Pt_{BN} \leq Pt_{max}\ \ AND\ RSCP_{BN} < RSCP'}$$

The transmission power is increased gradually to the $\boldsymbol{Pt'_{BN}}$ to prevent unnecessary battery drain and preserve power in case of having to revisit Phase 2 and trigger Stackelberg competition. In those cases where the $\boldsymbol{RSCP_{BN}}$ is still less than the $\boldsymbol{RSCP'}$ but their difference is either less than $\boldsymbol{Pt_{min}}$ or higher than $\boldsymbol{Pt_{max}}$, we deploy cost theory to set the BN transmission power $\boldsymbol{Pt'_{BN}}$:

$$\boldsymbol{TC = FC + VC} \tag{19}$$

where ***TC, FC*** and ***VC*** represent the total, fixed and variable cost respectively. We assign TC to $\boldsymbol{Pt'_{BN}}$, FC to either $\boldsymbol{Pt_{min}}$ or $\boldsymbol{Pt_{max}}$ accordingly and VC to the difference between $\boldsymbol{RSCP'}$ and $\boldsymbol{RSCP_{BN}}$:

$$\boldsymbol{FC = \{Pt_{min},\ Pt_{max}\}}$$

$$\boldsymbol{VC = RSCP' - RSCP_{BN}} \tag{20}$$

As the $\boldsymbol{RSCP'}$ is a constant value and the $\boldsymbol{RSCP_{BN}}$ is a variable we consider the derivative of $\boldsymbol{RSCP_{BN}}$ to calculate $\boldsymbol{Pt'_{BN}}$. When $\boldsymbol{FC = Pt_{min}}$:

$$\boldsymbol{Pt'_{BN} = \lim_{Pt_{min}\to Pt_{max}}\left(Pt_{min} + \left|\frac{\partial(VC)}{\partial(RSCP_{BN})}\right|\right)}$$

$$\boldsymbol{Pt'_{BN} = \lim_{Pt_{min}\to Pt_{max}}\left(Pt_{min} + \left|\frac{\partial\left(RSCP' - RSCP_{BN}\right)}{\partial(RSCP_{BN})}\right|\right)}$$

Since $\boldsymbol{Pt_{min}}$ =10 dB and $\boldsymbol{RSCP}$\` = −100 dB:

$$\boldsymbol{Pt'_{BN} = \lim_{10\to 20}\left(10 + \left|\frac{\partial\left(RSCP' - RSCP_{BN}\right)}{\partial(RSCP_{BN})}\right|\right)}$$

$$\boldsymbol{Pt'_{BN} = \lim_{10\to 20}\left(10 + \left|\frac{\partial\left(-100 - RSCP_{BN}\right)}{\partial(RSCP_{BN})}\right|\right)}$$

$$\boldsymbol{Pt'_{BN} = \lim_{10\to 20}(10 + |(0-1)|) = 11\ dB}$$

When $\boldsymbol{FC = Pt_{max}}$:

$$\boldsymbol{Pt'_{BN} = \lim_{Pt_{min}\to Pt_{max}}\left(Pt_{max} - \left|\frac{\partial(VC)}{\partial(RSCP_{BN})}\right|\right)}$$

$$\boldsymbol{Pt'_{BN} = \lim_{Pt_{min}\to Pt_{max}}\left(Pt_{max} - \left|\frac{\partial\left(RSCP' - RSCP_{BN}\right)}{\partial(RSCP_{BN})}\right|\right)}$$

Since $\boldsymbol{Pt_{max}}$ =20 dB and $\boldsymbol{RSCP}$\`=−100 dB:

$$\boldsymbol{Pt'_{BN} = \lim_{10\to 20}\left(20 - \left|\frac{\partial\left(RSCP' - RSCP_{BN}\right)}{\partial(RSCP_{BN})}\right|\right)}$$

$$\boldsymbol{Pt'_{BN} = \lim_{10\to 20}\left(20 - \left|\frac{\partial\left(-100 - RSCP_{BN}\right)}{\partial(RSCP_{BN})}\right|\right)}$$

$$\boldsymbol{Pt'_{BN} = \lim_{10\to 20}(20 - |0-1|) = 19\ dB}$$

Therefore, transmission power is controlled as:

$$\begin{aligned}
&\textbf{\textit{IF }} RSCP_{BN} \geq RSCP` \textbf{\textit{ THEN }} Pt'_{BN} = Pt_{BN} \textbf{\textit{ ELSE}}\\
&\textbf{\textit{IF }} RSCP_{BN} < RSCP` \textbf{\textit{ THEN}}\\
&\textbf{\textit{IF }} Pt_{min} < RSCP` - RSCP_{BN} < Pt_{max}\\
&\textbf{\textit{THEN }} Pt'_{BN} = RSCP` - RSCP_{BN} \textbf{\textit{ ELSE}}\\
&\textbf{\textit{IF }} RSCP` - RSCP_{BN} < Pt_{min} \textbf{\textit{ THEN}}\\
&Pt'_{BN} = \lim_{Pt_{min} \to Pt_{max}} \left(Pt_{min} + \left| \frac{\partial \left(-100 - RSCP_{BN}\right)}{\partial (RSCP_{BN})} \right| \right) \textbf{\textit{ELSE}}\\
&\textbf{\textit{IF }} RSCP` - RSCP_{BN} > Pt_{max} \textbf{\textit{ THEN}}\\
&Pt'_{BN} = \lim_{Pt_{min} \to Pt_{max}} \left(Pt_{max} - \left| \frac{\partial \left(-100 - RSCP_{BN}\right)}{\partial (RSCP_{BN})} \right| \right)
\end{aligned}$$

The new BN transmission power, Pt'_{BN}, is expressed as:

$$Pt'_{BN} = \begin{cases} Pt_{min}, & RSCP_{BN} \geq RSCP \\ RSCP` - RSCP_{BN}, & Pt_{min} < RSCP` - RSCP_{BN} < Pt_{max} \\ \lim\limits_{Pt_{min} \to Pt_{max}} \left(Pt_{min} + \left| \frac{\partial (-100 - RSCP_{BN})}{\partial (RSCP_{BN})} \right| \right), & RSCP` - RSCP_{BN} \leq Pt_{min} \\ \lim\limits_{Pt_{min} \to Pt_{max}} \left( Pt_{max} - \left| \frac{\partial (-100 - RSCP_{BN})}{\partial (RSCP_{BN})} \right| \right), & RSCP` - RSCP_{BN} \geq Pt_{max} \end{cases} \tag{21}$$

If an FUE receives more than one signal either from other FAPs and/or macrocell then phase 2 is executed again.

5. Experiment results and analysis

This section demonstrates the application of our proposed approach in managing interference using a mixture of actual measurements and simulation at a local college. After predicting the required number of FAPs, all FAPs are deployed at their optimal locations in open access mode. Each FAP can support upto 16 concurrent calls. Each device is deployed in co-channel mode with the macrocell, i.e. the spectrum is shared between them and the macrocell. Table 3 shows our femtocell experiment setup in relation to other reported setups in terms of cell radios, number of users, place of deployment, transmission power and configuration type.

Phase 1: Deployment Plan

Two experiments were carried out, one inside an anechoic chamber, and the other across the entire coverage area both inside and outside a building. The transmission power of each FAP whilst redirecting its antenna, and the precision of the mobile apps used for collecting measurements, i.e. Network Signal Info and Open Signal are assessed inside the anechoic chamber. Our results show that FAPs offer their lowest RSCP at 45°. Table 4 shows received signal power values at 45° intervals.

Table 3
Comparison between Base Stations.

Node	Cell Radios	Users	Location	Power output	configuration
Femto	**≤50 m**	**≤16**	**indoor**	**20 mW**	**Automatic**
Pico	100 m–300 m	≤64	Indoor/ Outdoor	200 mW–2 W	Automatic/ Manual
Micro	250 m–1 km	≤200	Outdoor	≤10 W	Automatic/ Manual
Macro	>1 km	>>200	Outdoor	40 W–100 W	Automatic/ Manual

Table 4
RSCP values at 45° intervals.

Angle	RSCP
0°	−55 dBm
45°	−62 dBm
90°	−55 dBm
135°	−61 dBm
180°	−55 dBm
225°	−60 dBm
270°	−55 dBm
315°	−58 dBm
360° = 0°	−55 dBm

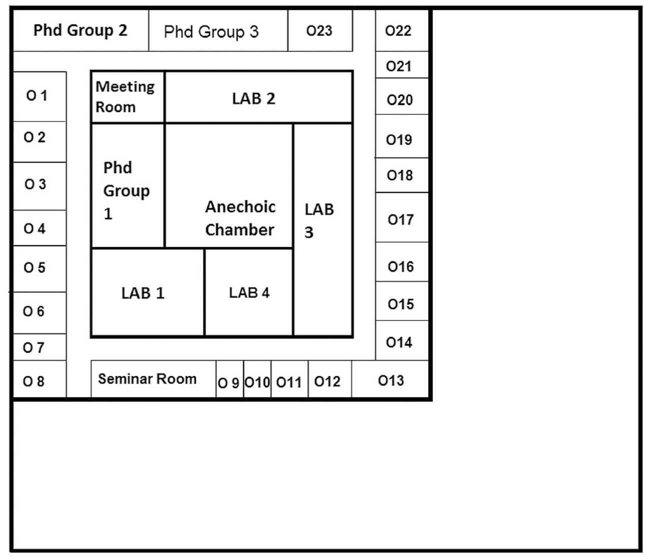

Fig. 10. Area Layout.

Taking measurements of the entire coverage area helps with predicting the number of FAPs required and with setting both the RSCP and distance thresholds. Fig. 10 shows area layout. The coverage area used in our experiment is a one floor building surrounded by open space which thus requires both indoor and outdoor deployment. The walls inside the building were tested and were classified into two types based on their penetration loss values. Light walls exhibit penetration loss of 4 dB each. Heavier walls exhibit penetration loss of 8 dB each. The RSCP from the macrocell were also tested randomly, both indoor and outdoor, and the highest received signal was −100 dB so this was set as the RSCP threshold. When an FUE is on the move and at a distance of 30 m to the FAP, the RSCP decreases so 30 m was set as the distance threshold in order to prevent a signalling overhead as the FAP will need to boost its transmission power to cover a larger distance. The threshold multipath is calculated at 110 dB. Both the width and length of the area shown on Fig. 2 is 60 m. Therefore, the required number of FAPs (Eq. (1)):

$$NoFAPs = \frac{(L \times W)}{(D')^2} = \frac{(60 \times 60)}{30^2} = 4 \textit{ FAPs}$$

Table 5 shows the actual measurements that will be simulated.

Step 1: Indoor deployment plan

The building is tested in eight angle directions at 5 m intervals as shown on Fig. 11 and the weakest RSCP from the macrocell and its location in each direction is recorded on Table 6. FAP_1 is installed at the location of the weakest signal, C, from the macrocell that offers the highest possible coverage (Eq. (4)):

Table 5
Simulation input.

Parameter	Value
Area Width	60 m
Area Length	60 m
Floor Width (W_{Floor})	40 m
Floor Length (L_{Floor})	45 m
Light Wall penetration loss (LW)	4 dB
Path Loss at reference point (PL_r)	−50 dB
FAP to reference point distance (R)	1 m
Heavy Wall penetration wall (HW)	8 dB
Pathloss model (EDS)	K = 2.17
Initial transmission power (P_t)	10 dB
Number of FAPs (NoFAPs)	4
Number of FUEs (NoFUEs)	7
Distance threshold (D′)	30 m
Received power threshold (RSCP′)	−100 dB

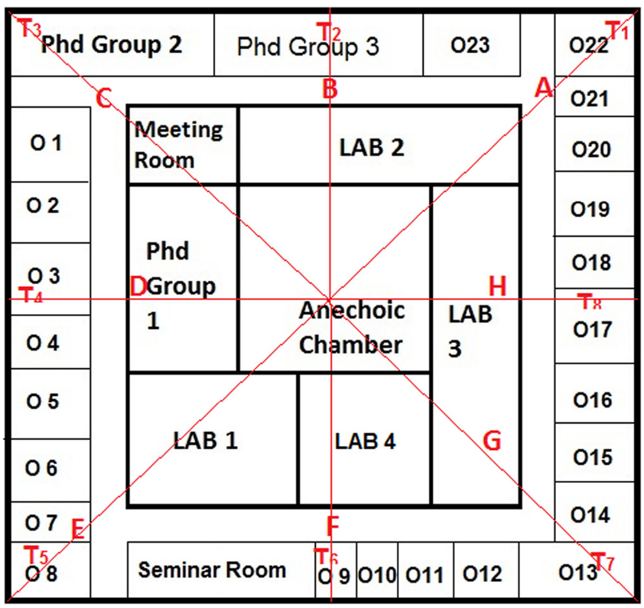

Fig. 11. RSCP testing.

Table 6
Macrocell RSCP.

Location	$RSCP_1$	$RSCP_2$	RSCP
A	−100 dB	−100 dB	−100 dB
B	−101 dB	−103 dB	−102 dB
C	xxxxx	xxxxx	xxxxx
D	−105 dB	−105 dB	−105 dB
E	−100 dB	−100 dB	−100 dB
F	−103 dB	−107 dB	−105 dB
G	xxxxx	xxxxx	xxxxx
H	xxxxx	xxxxx	xxxxx

$$FAP_1 = \begin{cases} \boldsymbol{Min}\ \{\boldsymbol{RSCP}_{macro}\} = \boldsymbol{C}, \boldsymbol{G}, \boldsymbol{and}\ \ \boldsymbol{H} \\ \boldsymbol{Max}\ \{\boldsymbol{coverage}\} = \boldsymbol{C} \end{cases}$$

Testing commences once again and continues likewise to locate the weakest RSCP from FAP_1. Fig. 12 shows the location of the eight weakest RSCPs at one of which FAP_2 is installed. Table 7 records the weakest RSCP values and their distance from FAP_1. FAP_2 is deployed at location B as shown on Fig. 13. The deployed FAPs do not provide coverage for the whole floor because the anechoic chamber absorbs all passing signals. Providing service out of the anechoic chamber is not feasible thus this room is not considered for installation of another FAP.

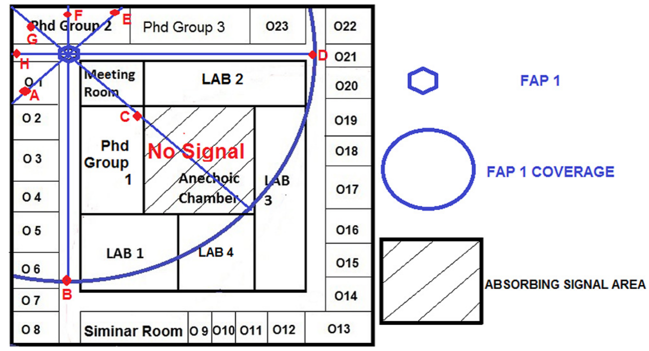

Fig. 12. Weakest RSCPs from FAP_1.

Table 7
Weakest RSCPs from FAP_1.

Location	Distance from FAP_1	RSCP value
A	5 m	−81 dB
B	30 m	−97 dB
C	10 m	−85 dB
D	30 m	−93 dB
E	10 m	−84 dB
F	5 m	−79 dB
G	5 m	−80 dB
H	5 m	−81 dB

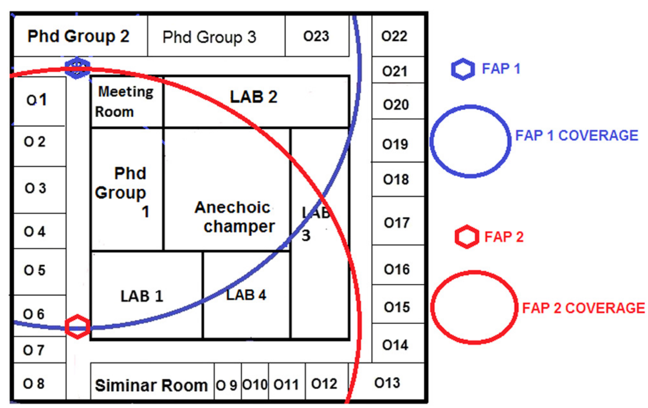

Fig. 13. Deployment of FAP_2.

Step 2: Outdoor deployment plan

The remaining two FAPs are installed outdoors. Fig. 14 shows the test plan for the outdoors. Outdoors testing is carried out at 3 locations. Deployment of FAP_3 is carried out at T_{11} as shown on Fig. 15 as there is no RSCP at this location. Testing commences once again in three directions as shown on Fig. 16 and continues likewise to locate the weakest RSCP from FAP_3. Table 8 records the RSCP value at locations A, B and C. FAP_4 is deployed at location A. Fig. 17 shows the entire coverage area after deployment of the four FAPs.

Phase 2: Finding Best Nodes (FBN)

In our experiment, we consider the existence of 7 FUEs. Fig. 18 shows their locations. Two FUEs are in the interference area of FAP_1 and FAP_2 as shown on Fig. 19. Deploying the parameters of Table 4 (Eq. (7)):

$$\boldsymbol{PL} = \mathbf{50} + \mathbf{2.17} \times \mathbf{10}\ \mathbf{log_{10}}\,(\boldsymbol{d}) + \sum_{\boldsymbol{w}}^{\boldsymbol{n}} (\mathbf{4}^{*}\boldsymbol{n} + \mathbf{8}^{*}\boldsymbol{n})$$

The FMS identifies candidate BNs for each FUE. RSCPs are compared

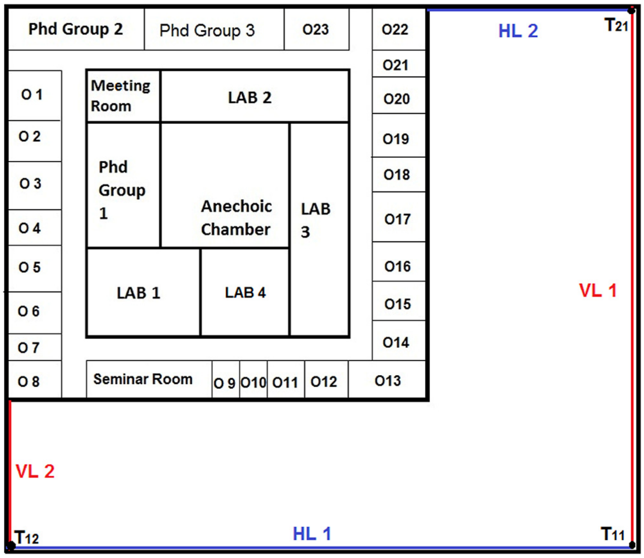

Fig. 14. Outdoor test locations.

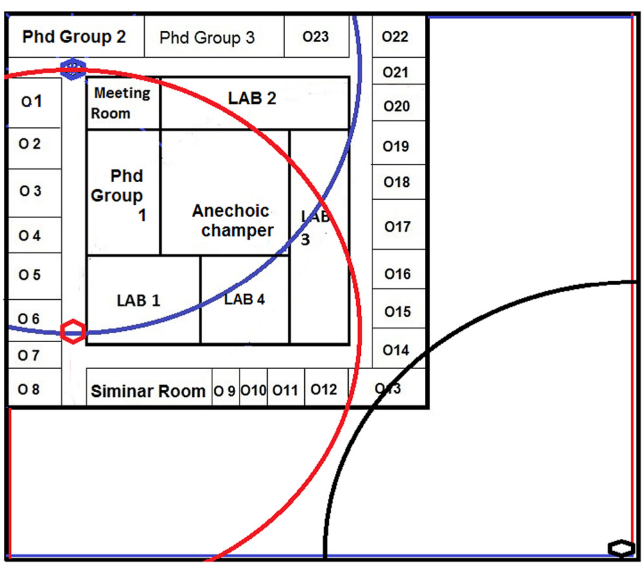

Fig. 15. Deployment of FAP_3 outdoors.

first followed by multipath then distance. The distance between FUE_1 and FAP_1 is 19 m and between FUE_1 and FAP_2 is 17 m. Fig. 20 shows the RSCP detected. Despite FUE_1 being closer to FAP_2 the best node is FAP_1 because it is the node that provides the FUE_1 with the highest RSCP. Distance and multipath are not considered as the RSCP value has priority over all other factors. FMS connects FUE_1 to FAP_1 and if FUE_1 moves away all other factors are considered again and the new best FAP is identified again. In the case of FUE_1 moving to a place with no signal, BNKC algorithms will be applied. Table 9 shows the RSCP values from each FAP. Table 10 records the results for the two distances of 17 m and 19 m.

Distances between the macrocell and user equipment are not measured and the multipath value are not predicted due to the unknown macrocell transmission value. This does not represent an exception to our proposed algorithms since all RSCPs from the macrocell are less than −100 dB which is less than the RSCP\`. FAP_1 is the best node for FUE_1 (Eq. (11)):

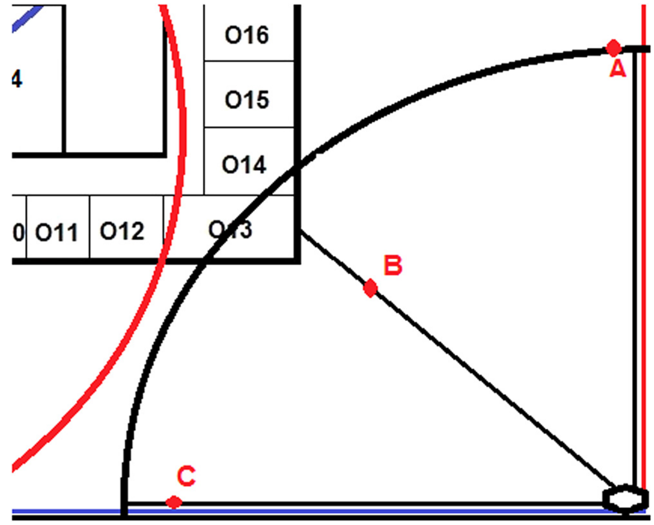

Fig. 16. Testing from FAP_3.

Table 8
Weakest RSCP from FAP_3.

Location	Distance from FAP_1	RSCP value
A	30 m	−79 dB
B	24 m	−71 dB
C	28 m	−73 dB

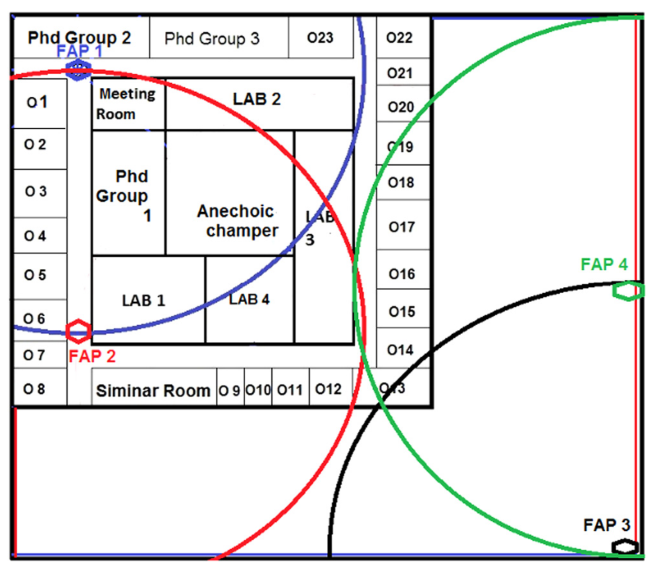

Fig. 17. Coverage area after deployment of the four FAPs.

$$BN_{FUE_1}^{RSCP_1} = \begin{cases} \boldsymbol{Max}\left\{\boldsymbol{RSCP}_1\right\} = -83.42 \text{ dB} \\ \boldsymbol{PL}_i^* \\ \varnothing \end{cases}$$

FMS which controls the connection between an FUE and its FAP blocks the rest of the nodes to avoid both co-tier and cross-tier interference. FUE_2 is located approximately 15 m away from each FAP (Eq. (14)):

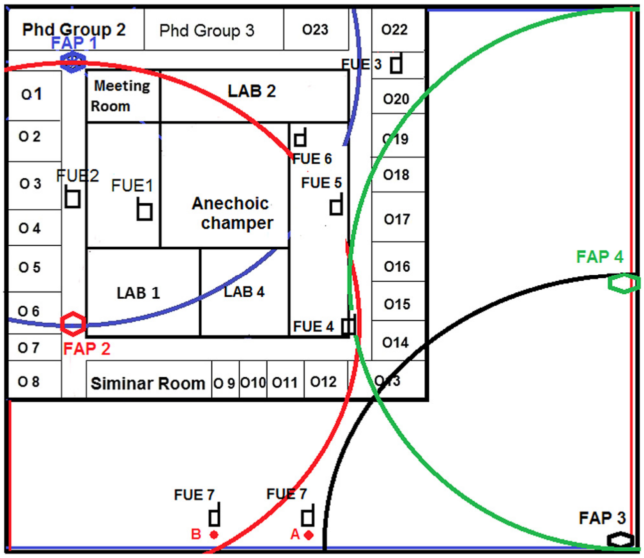

Fig. 18. FUEs locations.

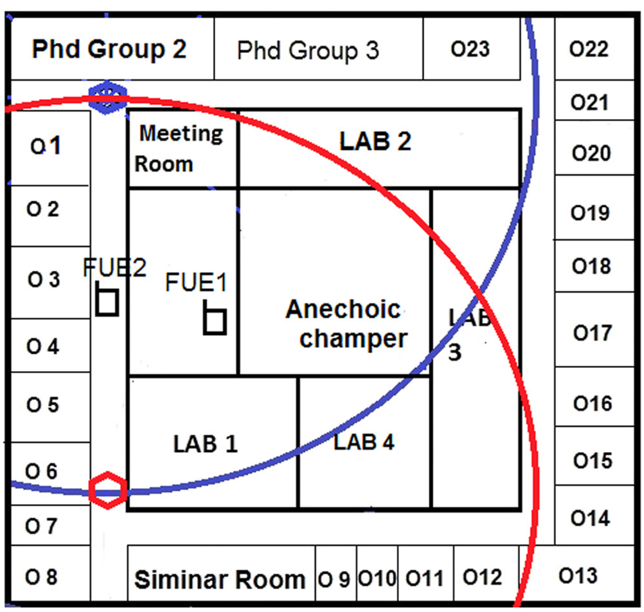

Fig. 19. FUEs in the interference area of FAP_1 and FAP_2.

$$BN_{FUE_2} = \begin{cases} \mathbf{Max}\left\{\mathbf{RSCP}_{1,2}\right\} = -69.78\ \mathbf{dB} \\ \begin{cases} \mathbf{Min}\left\{\mathbf{PL}_{1,2}\right\} = 79.78\ \mathbf{dB} \\ \begin{cases} \mathbf{Min}\left\{\mathbf{D}_{1,2}\right\} = 15\ \mathbf{m} \\ \mathbf{Stac}^{*} \\ \varnothing \end{cases} \\ \varnothing \end{cases} \\ \varnothing \end{cases}$$

Table 11 records the results for $\mathbf{FUE_2}$

The macrocell is not considered as it offers the lowest power whereas FAP_1 and FAP_2 provide higher power to the user equipment than the RSCP`. Stackelberg is applied to prevent a random choice between these two FAPs. The first mover is always the FAP which has been installed first. As we have a prior knowledge about the demand, the curve demand

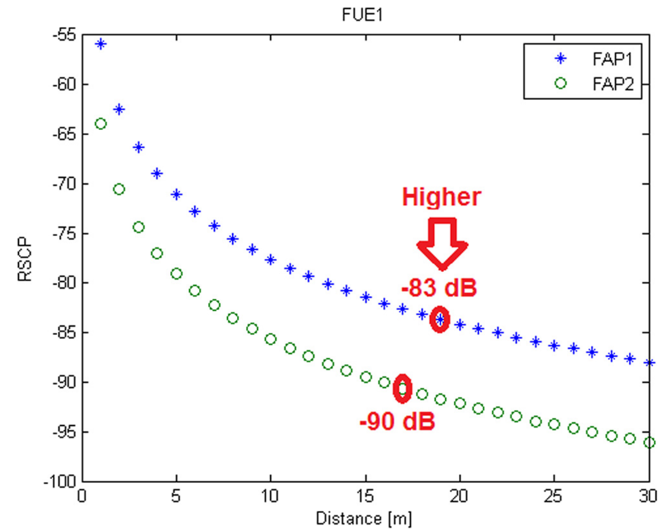

Fig. 20. FUE_1 RSCPs.

Table 9
FUE_1 received power from both FAPs.

Distance	$RSCP_{FAP_1}$	$RSCP_{FAP_2}$
5 m	−71.17 dB	−79.17 dB
10 m	−77.70 dB	−85.70 dB
15 m	−81.58 dB	−89.52 dB
17 m	−82.70 dB	**−90.20 dB**
19 m	**−83.42 dB**	−91.75 dB
20 m	−84.23 dB	−92.23 dB
25 m	−86.34 dB	−94.34 dB
30 m	−88.05 dB	−96.05 dB

Table 10
RSCP, D, and PL values from all nodes for FUE_1.

Node	RSCP	D	PL
FAP_1	−83.42 dB	19 m	93 dB
FAP_2	−90.20 dB	17 m	100 dB
Macrocell	−105 dB	xxx	xxx

Table 11
RSCP, D, and PL values from all nodes for FUE_2.

Node	RSCP	D	PL
FAP_1	−69.78 dB	15 m	79.78 dB
FAP_2	−69.78 dB	15 m	79.78 dB
Macrocell	−105 dB	xxx	xxx

is (Eq. (16)):

$$\mathbf{P} = \mathbf{20} - \mathbf{0.5}\left(\boldsymbol{Pt}_{\boldsymbol{FAP_i}}\right)$$

With Stackelberg competition Pt_{FAP_1} is set to the maximum transmission power of 20 dB whereas Pt_{FAP_2} is set to 10 dB. Figs. 21 and 22 show the shift of power before and after using Stackelberg. FAP_1 offers FUE_2 a higher value RSCP so it becomes its best node. Tables 12 and 13 record the RSCP values at 5 m intervals before and after applying Stackelberg.

Phase 3: Best Node Keep Connected (BNCN)

FUE_3's $RSCP_{BN}$ is higher than the threshold but it is located more than 30 m from FAP_1, FUE_4 receives a signal that is lower than the RSCP`, $FUE_5$ receives a poor signal that is more than 10 dB less than the RSCP` and FUE_6 receives a poor signal that is more than 20 dB less

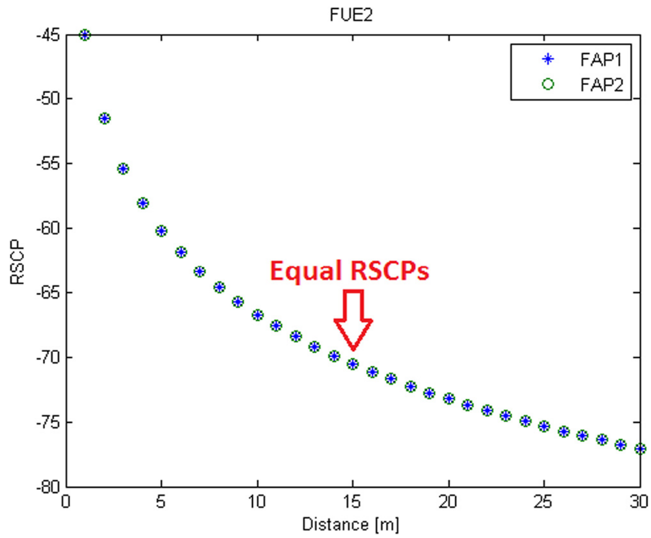

Fig. 21. RSCPs values from both FAPs before Stackelberg.

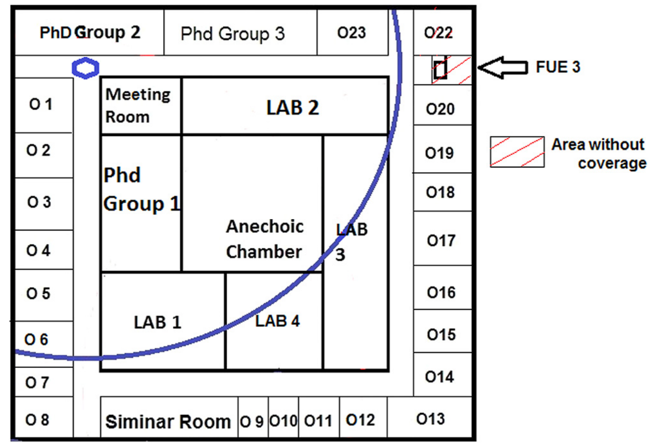

Fig. 23. FUE_3 in the coverage area.

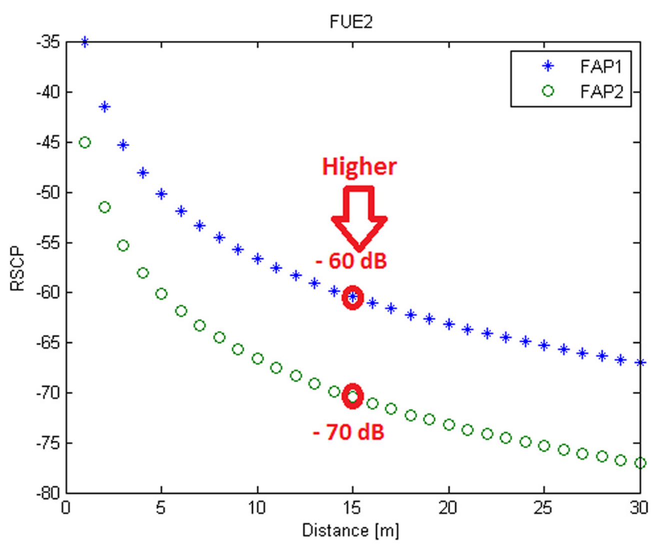

Fig. 22. RSCPs values from each FAP after Stackelberg.

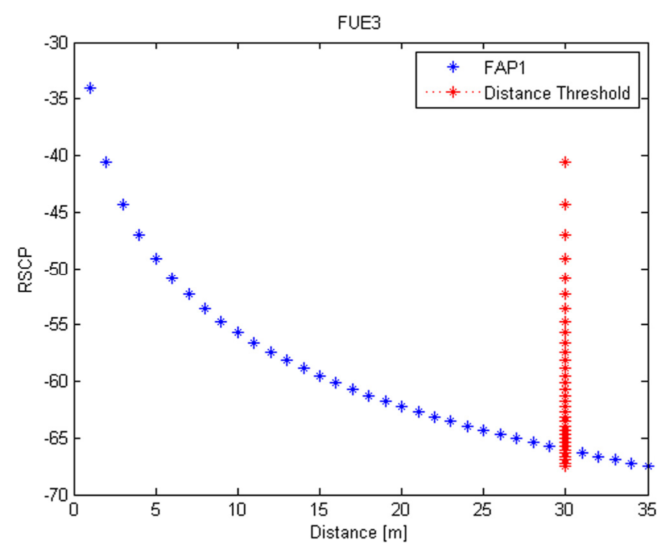

Fig. 24. RSCPs between FUE_3 and FAP_1.

Table 12
Initial RSCP values received by FUE_2.

Distance	$RSCP_{FAP_1}$	$RSCP_{FAP_2}$
5 m	−58.06 dB	−58.06 dB
10 m	−65.70 dB	−65.70 dB
15 m	**−69.87 dB**	**−69.87 dB**
20 m	−72.75 dB	−72.75 dB
25 m	−74.95 dB	−74.95 dB
30 m	−76.73 dB	−76.73 dB

Table 13
RSCP values received by FUE_2 after Stackelberg.

Distance	$RSCP_{FAP_1}$	$RSCP_{FAP_2}$
5 m	−48.06 dB	−58.06 dB
10 m	−55.70 dB	−65.70 dB
15 m	**−59.87 dB**	**−69.87 dB**
20 m	−62.75 dB	−72.75 dB
25 m	−64.95 dB	−74.95 dB
30 m	−66.73 dB	−76.73 dB

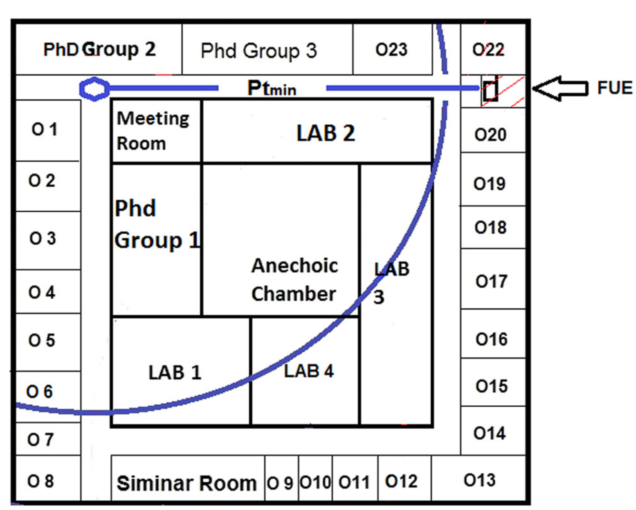

Fig. 25. Connection between FUE_3 and FAP_1.

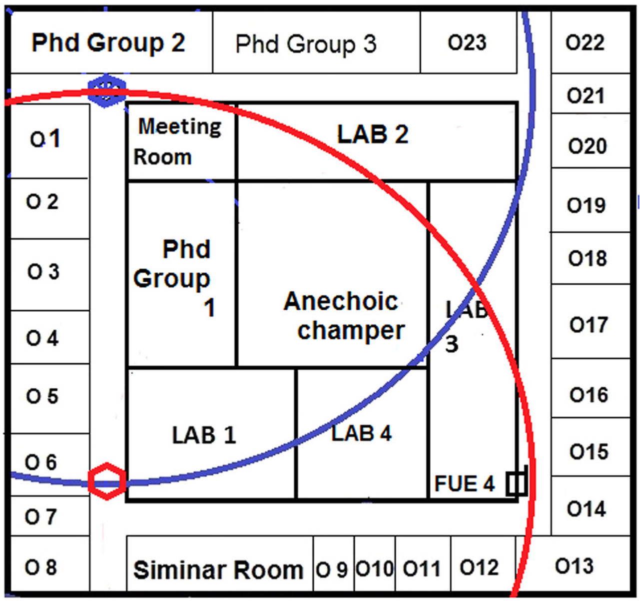

Fig. 26. FUE_4 in FAP_2's coverage area.

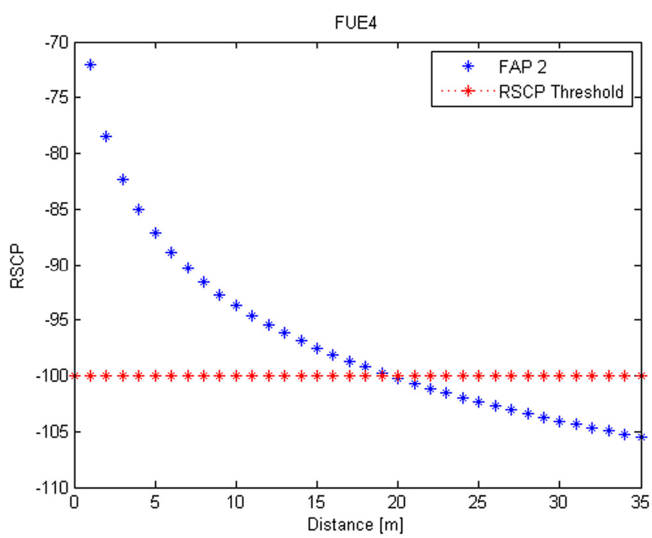

Fig. 27. FUE_4 RSCP values from FAP_2.

than the RSCP`. Fig. 23 shows the location of FUE_3 inside the coverage area but without coverage from the macrocell but it receives a strong RSCP from FAP_1.

FUE_3's $RSCP_{BN}$ values are predicted (Eqs. (7) and (8)):

$$\boldsymbol{RSCP} = \mathbf{20} - \boldsymbol{PL}$$

$$\boldsymbol{PL} = \mathbf{50} + \mathbf{2.17} \times \mathbf{10}\ \mathbf{log_{10}}\,(\mathbf{32}) + \sum_{w}^{n} \left(\mathbf{4}^{*}\mathbf{1} + \mathbf{8}^{*}\mathbf{0}\right)$$

FUE_3 is approximately 32 m away from FAP_1 which means the distance between FUE_3 and FAP_1 is 2 m longer than D`. However, according to the results shown in Fig. 24, the RSCP is −66.36 dB which is higher than the RSCP`. Based on the BNKC algorithm the distance threshold is ignored to provide service for this FUE without any change in the transmission power to prevent any potential interference. Fig. 25 shows FUE_3 connecting to FAP_1 which is similar to beamforming without creating null power to other FUEs.

FUE_4 is located where there is no received power from the macrocell and there is loss which decreases the quality of connection between FAP_2 and FUE_4. FUE_4 is approximately 30 m away from FAP_2. Fig. 26 shows the location of FUE_4. As can be seen on Fig. 27 the RSCP at the 30 m distance is about −103.73 dB. This means the difference between the $RSCP_{BN}$ and RSCP` is less than the Pt_{min}. After maximising the transmission power to about 11 dB the RSCP is slightly increased. Fig. 28 shows the difference between RSCPs values before and after increasing the transmission power. Table 14 records the difference in RSCP values before and after maximising transmission power. FUE_5 is located 35

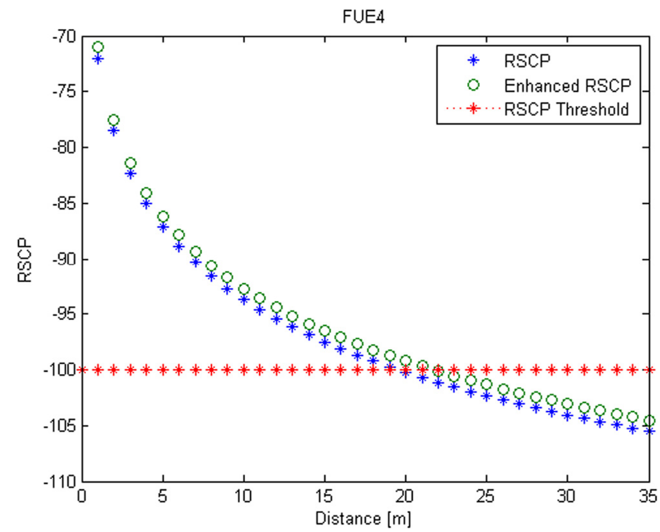

Fig. 28. RSCPs values before and after increase.

Table 14
RSCPs values.

Distance	Initial RSCP	RSCP after maximising transmission power
5 m	−85.07 dB	−84.07 dB
10 m	−90.34 dB	−89.34 dB
15 m	−96.87 dB	−95.87 dB
20 m	−99.75 dB	−98.75 dB
25 m	−101.95 dB	−100.95 dB
30 m	**−103.73 dB**	**−102.73 dB**

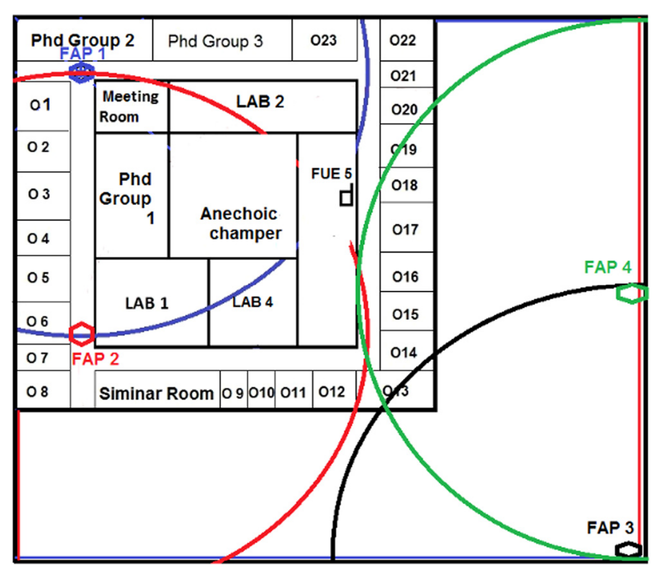

Fig. 29. FUE_5's location.

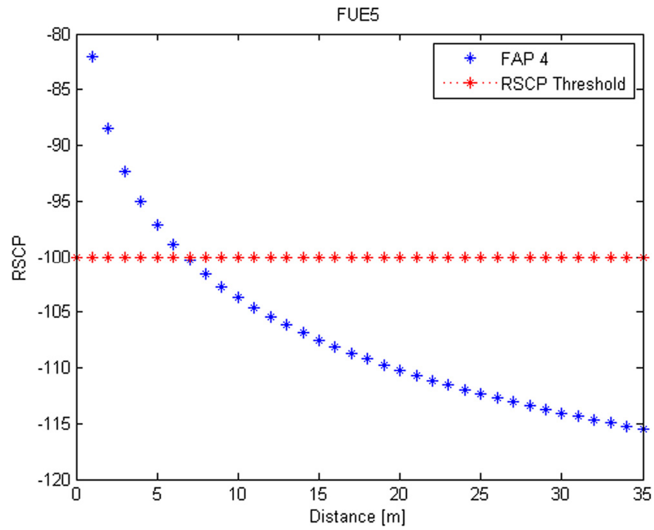

Fig. 30. FUE_5 RSCP value from FAP_4.

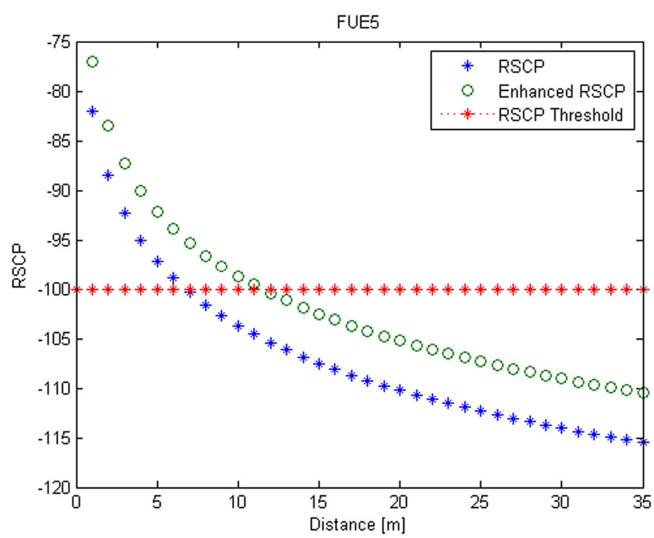

Fig. 31. RSCP before and after resetting Pt_{BN}.

Table 15
RSCPs values.

Distance	Initial RSCP	RSCP after maximising transmission power
5 m	−95.07 dB	−90.07 dB
10 m	−102.71 dB	−97.71 dB
15 m	−106.87 dB	−101.87 dB
20 m	−109.75 dB	−104.75 dB
25 m	−111.95 dB	−106.95 dB
30 m	−113.73 dB	−108.73 dB
35 m	**−115.23 dB**	**−110 dB**

m away from FAP_4 where there is no RSCP from either the macrocell, FAP_1 or FAP_2 as it is located behind the anechoic chamber. Fig. 29 shows the location of FUE_5. As FAP_4 is the only FAP that can serve FUE_5's location, it is connected to that FUE regardless of D` in order to mitigate the probability of outage. Fig. 30 shows the RSCP at that location. The $RSCP_{BN}$ is about −115 dB so the difference between this value and RSCP` is about 15 dB. Based on our BNKC (Eq. (18)):

$$\boldsymbol{Pt'_{BN}} = \mathbf{-100\ dB - (-115) = 15\ dB}.$$

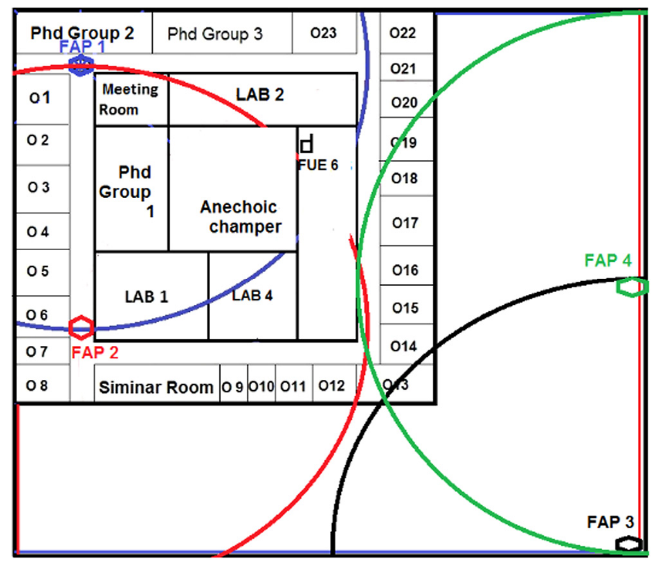

Fig. 32. FUE_6's location behind the anechoic chamber.

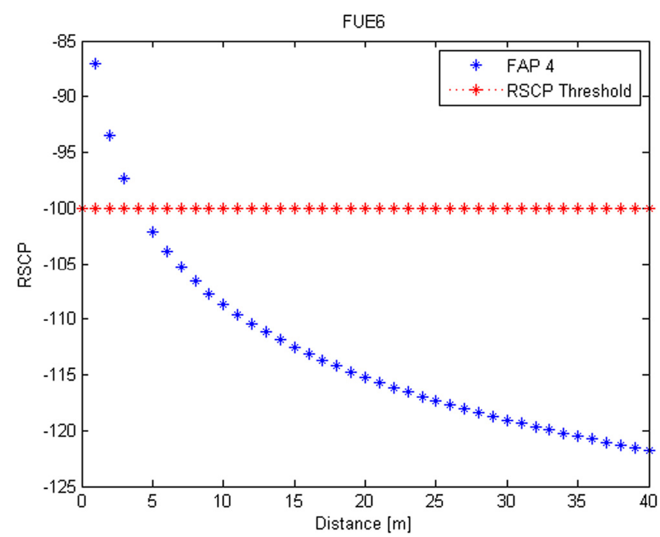

Fig. 33. FUE_6's RSCP values from FAP_4.

Fig. 31 and Table 15 show the difference before and after resetting $\boldsymbol{Pt_{BN}}$. FUE_6 is located 40 m away from FAP_4 and there is no signal received from other nodes because it is located behind the anechoic chamber. Fig. 32 shows the location of FUE_6. FUE_6 is now connected to FAP_4 with a 15 dB transmission power because it is also connected to FUE_5. Fig. 33 illustrates the RSCP at that location. The $RSCP_{BN}$ is about −122 dB so the difference to RSCP` is higher than Pt_{max}. Based on our BNKC the transmission power is set at 19 dB. As a result, the RSCP is raised by 4 dB. Fig. 34 and Table 16 show the difference before and after resetting $\boldsymbol{Pt_{BN}}$.

5.1. BNKC to FBN

Here, we consider the case when an FUE on the move receives another signal. Fig. 35 shows FUE_7 moving from location A to B where there is no macrocell coverage. At A FUE_7 receives a signal from FAP_3 which is set as its BN. Fig. 36 shows the RSCP values from FAP_3.

When FUE_7 moves 31 m away from FAP_3 where it receives a strong signal from FAP_3 which equals to −72 dB, then based on our BNKC,

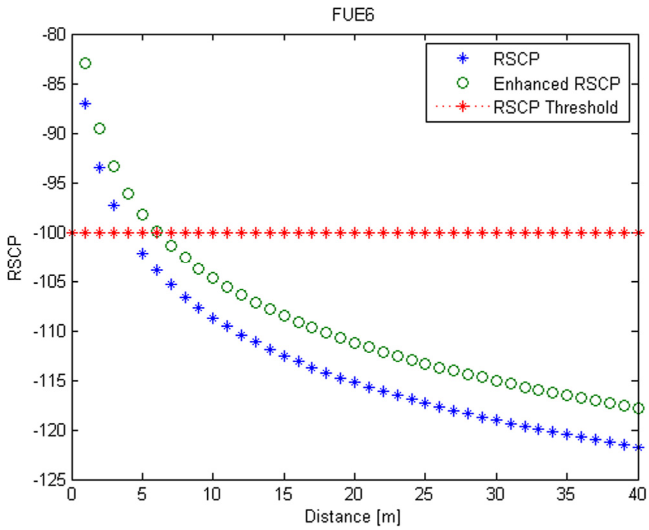

Fig. 34. RSCP before and after resetting Pt_{BN}.

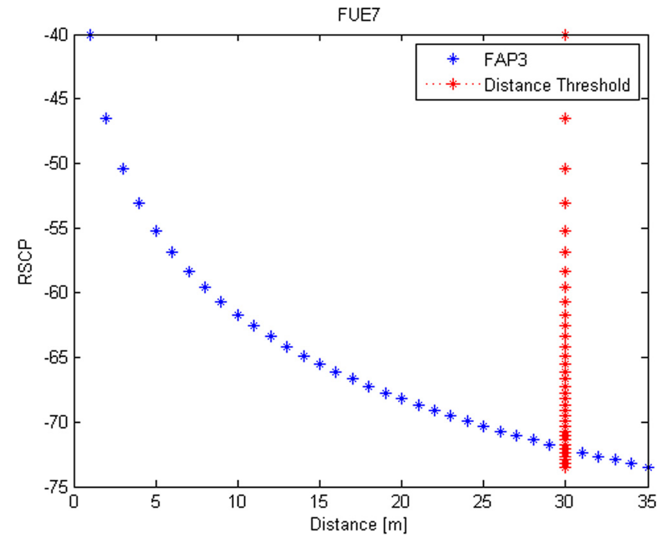

Fig. 36. RSCPs from FAP_3.

Table 16
RSCPs values.

Distance	Initial RSCP	RSCP after maximising transmission power
5 m	−100 dB	−96 dB
10 m	−107.71 dB	−93.71 dB
15 m	−111.87 dB	−107.87 dB
20 m	−115 dB	−111 dB
25 m	−117 dB	−113 dB
30 m	−118.7 dB	−114.7 dB
35 m	−120 dB	−116 dB
40 m	**−122 dB**	**−118 dB**

Table 17
FUE_7 RSCPs from both FAPs.

Distance	$RSCP_{FAP_2}$	$RSCP_{FAP_3}$
5 m	−64 dB	−53 dB
10 m	−71.71 dB	−60.71 dB
15 m	−75.87 dB	−64.87 dB
20 m	−78.75 dB	−67.75 dB
25 m	−81 dB	−70 dB
29 m	**−82.40 dB**	−71.40 dB
37 m	−84.77 dB	**−73.77 dB**
40 m	−85.35 dB	−74.35 dB

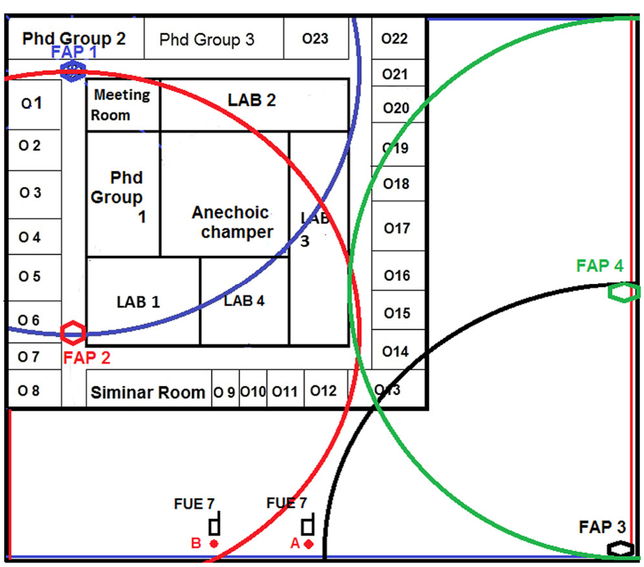

Fig. 35. FUE_7 on the move.

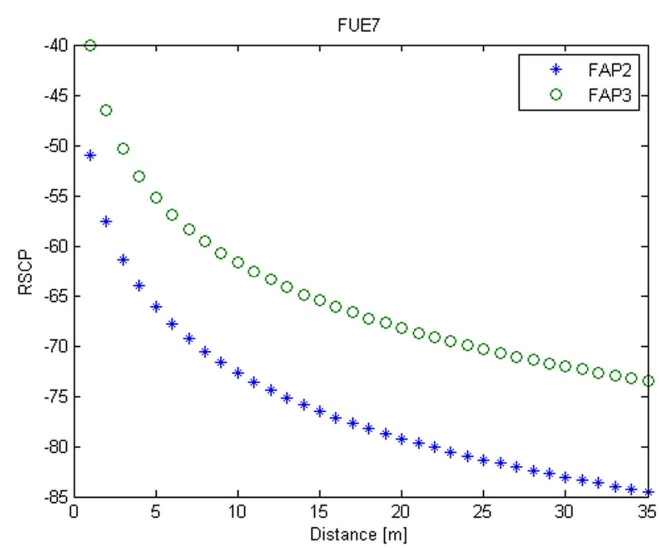

Fig. 37. RSCPs from both FAPs.

there is no change in transmission power. When FUE_7 moves from A to B where it receives another signal from FAP_2 then phase 2, FBN, is revisited. Fig. 37 shows the RSCP from both FAPs at location B. As there is no coverage from macrocell when moving A to B, the RSCP` and D` are not considered. B is approximately 29 m away from FAP_2 and 37 m away from FAP_3. However, the best node is FAP_3 as it offers the highest RSCP. There is loss between FAP_2 and FUE_7. Table 17 records the results for each FAP.

Revisiting FBN (Eq. (11)):

$$BN_{FUE_7}^{RSCP_3} = \begin{cases} \boldsymbol{Max}\left\{\boldsymbol{RSCP}_3\right\} = -73.77\ \textbf{dB} \\ \boldsymbol{PL}_i^* \\ \varnothing \end{cases}$$

Although FAP_2 may boost its transmission power and be closer to FUE_7, the best node for FUE_7 is FAP_3. The transmission power value for each FAP is predicted as $Pt_{FAP_1} = 20$ dB, $Pt_{FAP_2} = 11$ dB, $Pt_{FAP_3} = 10$ dB $Pt_{FAP_4} = 19$ dB. Table 18 shows all user equipment and their BNs.

Table 18
User equipment and their BNs.

UE	BN	Pt (dBm)	RSCP (dBm)	PL (dBm)	D
FUE_1	FAP_1	10	−83.42	93	19 m
FUE_2	FAP_1	20	−59.78	80	15 m
FUE_3	FAP_1	20	−66.36	86	32 m
FUE_4	FAP_2	11	−102.73	114	30 m
FUE_5	FAP_4	15	−110	125	35 m
FUE_6	FAP_4	19	−118	137	40 m
FUE_7 @ A	FAP_3	10	−72	82	31 m
FUE_7 @ B	FAP_3	10	−73.77	84	37 m

5.2. Complexity analysis of our approach

To consider the complexity of the three-phase approach each phase process is drawn as a decision tree as shown on Fig. 38 to estimate the longest path in each phase and thereby calculate its complexity. Phase 1 is carried out once only so its complexity function is as follows:

$$O_{Ph_1}(n) = n + C_{Ph_1} \tag{22}$$

where $O_{Ph_1}(n)$ denotes the complexity level, n is the number of operations, and $C_{Ph_1} = 0.74$. Phase 2 maybe highly iterative so its complexity function is as follows:

$$O_{Ph_1}(n) = n^2 + C_{Ph_2} \tag{23}$$

where $C_{Ph_2} = 0.6$.

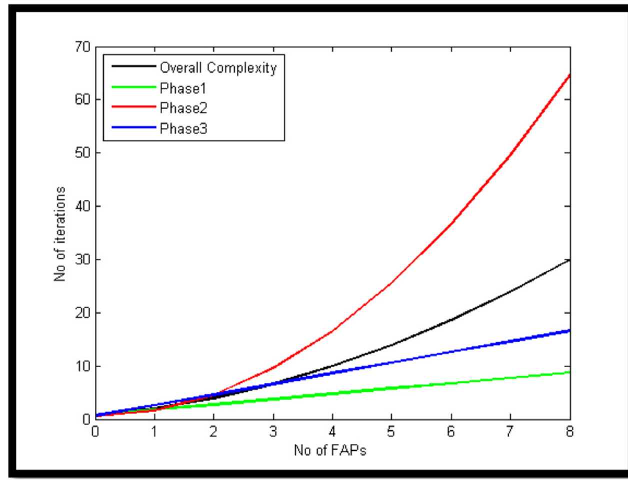

Fig. 39. Three-phase complexity.

Table 19
The Hybrid approach vs the approach in [9].

UE	BN	Pt (hybrid)	RSCP (hybrid)	Pt [9]	RSCP [9]	D
FUE_4	FAP_2	11 dB	−102.73 dB	2 dB	−111 dB	30 m
FUE_5	FAP_4	15 dB	−110 dB	7 dB	−118 dB	35 m
FUE_6	FAP_4	19 dB	−118 dB	7 dB	xxx	40 m

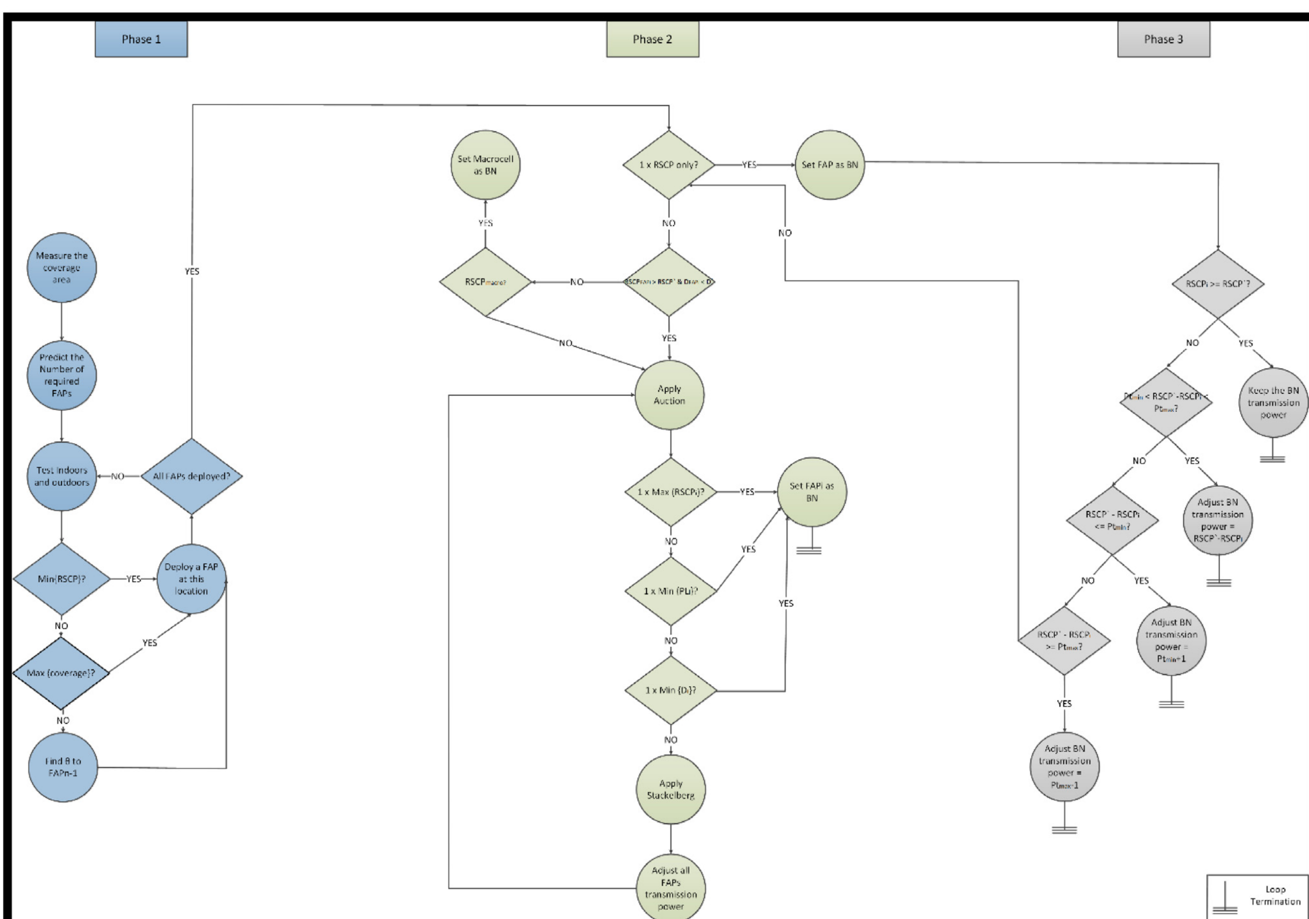

Fig. 38. Three-phase decision tree.

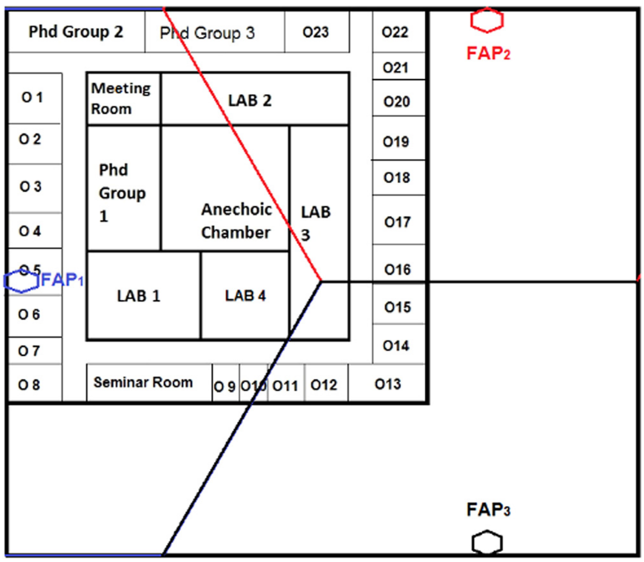

Fig. 40. Hexagonal coverage after deploying FAPs [29].

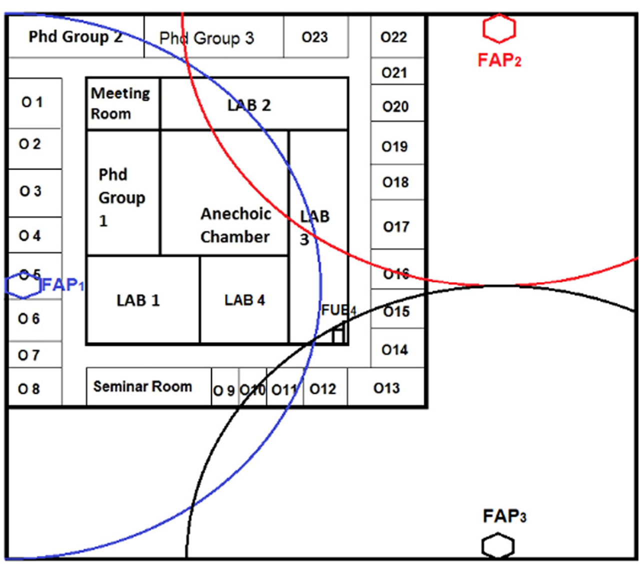

Fig. 41. Radius coverage after deploying the FAPs [29].

Table 20
FUE_4-The Hybrid approach vs the approach in [29].

FUE_4	BN	Pt	RSCP	PL	D
Hybrid Approach	FAP_2	11 dB	−102.73 dB	114 dB	30 m
Approach in [29]	xxx	xxx	xxx	xxx	xxx

Phase 3 is also iterative but with a smaller number of iterations so its complexity function is as follows:

$$O_{Ph_1}(n) = n \times 2 + C_{Ph_3} \tag{24}$$

where $C_{Ph_3} = 0.6$.

Fig. 39 shows the level of complexity level for each phase and the overall complexity, with phase 2 achieving the highest level in comparison to the other two phases, partly due to the number of parameters in consideration during this phase and partly due to the higher number of iterations. Although during phase 1 the number of parameters considered are higher in comparison to phase 3, phase 3's complexity is higher, largely due to the number of iterations. What the

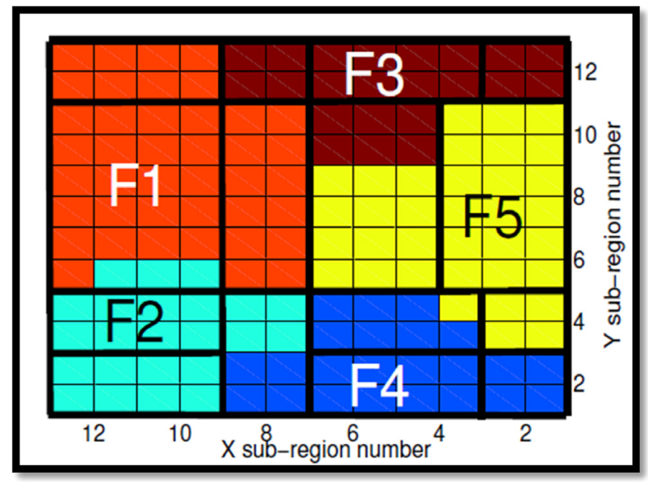

Fig. 42. FAPs deployment [30].

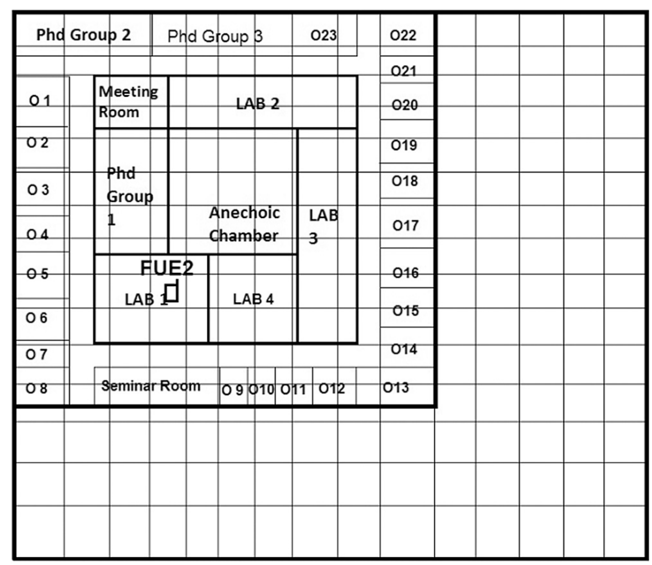

Fig. 43. College divided into sub-regions.

complexity graphs reveals is that the number of iterations increases exponentially in relation to the number of FAPs, especially during phase 2. The overall complexity rises proportionally to the number of FAPs which suggests a medium level of complexity.

6. Comparative evaluation to other approaches

In this section, we deploy techniques that have been reported in our literature review in the grounds of the same local college and then compare these to the hybrid approach. In [9] FTN and TAPB algorithms are proposed to resolve interference. The aim of this approach is to identify the node that causes interference and then minimise the transmission power of that node. The authors do not propose any algorithms to locate FAPs at optimum locations. They assume that their algorithms are suitable regardless of the number of FAPs and their locations. The authors suggest that the FAPs with higher number of neighbours should decrease their transmission power. Thus, the new transmission power for the trouble node is equal to the common transmission power minus the difference between the lowest received power by any FUE and the lowest received power from the trouble node FAP. We apply this approach inside the college and then compare it to our own hybrid

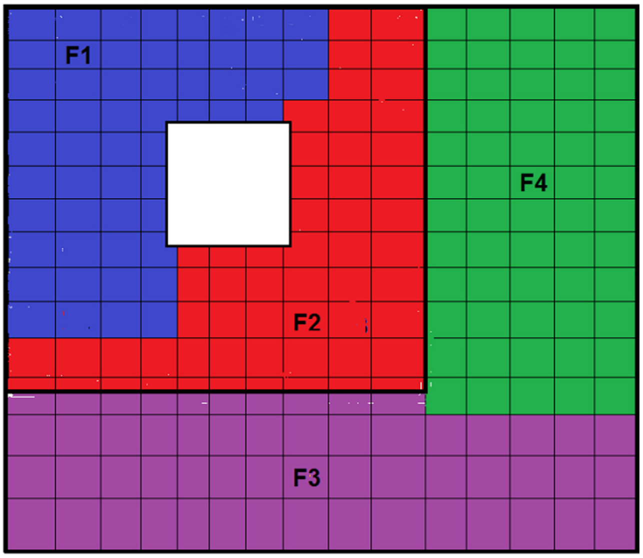

Fig. 44. FAPs deployed in college [30].

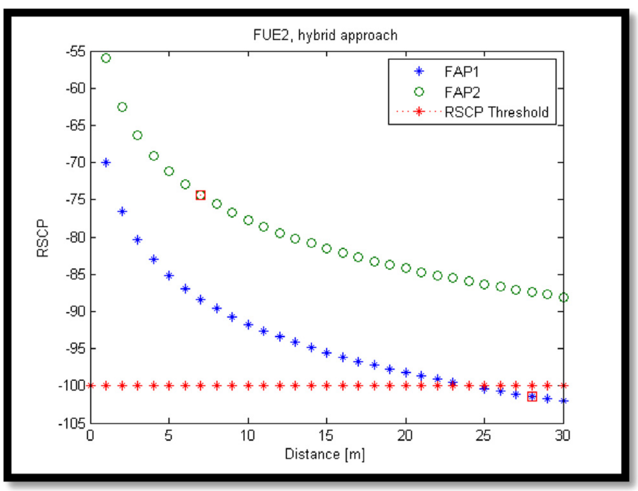

Fig. 45. RSCP values with the hybrid approach.

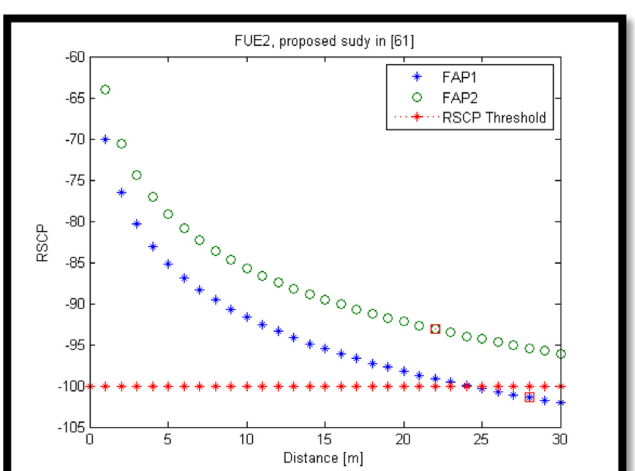

Fig. 46. RSCP values with [30].

Table 21
FAP_1 and FAP_2 - The Hybrid approach vs the approach in [30].

Node	RSCP (hybrid)	D (hybrid)	RSCP [30]	D [30]
FAP_1	−101 dB	28 m	−101 dB	28 m
FAP_2	−74 dB	7 m	−93 dB	22 m

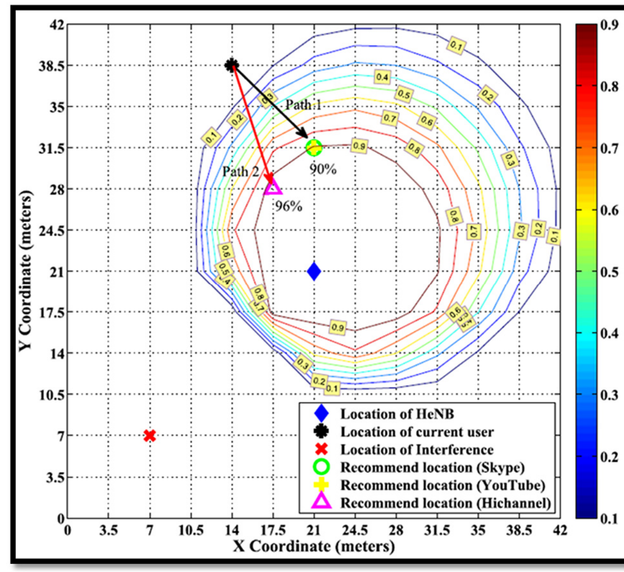

Fig. 47. User placement using ushering mechanism.

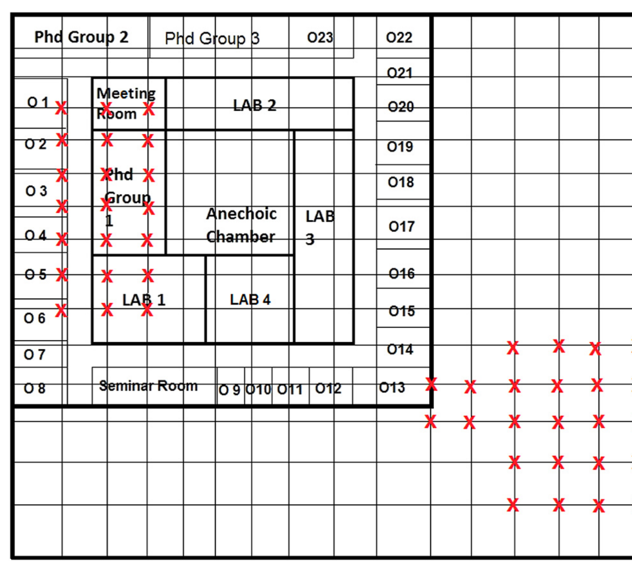

Fig. 48. The interference area using ushering mechanism.

approach. As the FAPs with the highest number of neighbours are FAP_2 and FAP_4 (see Fig. 17) we decrease their transmission power and set their new transmission power to obtain the difference in RSCP before and after. We start by calculating the new transmission power for these FAPs. Firstly, we test the weakest received signal by all FUEs, i.e. −118 dB. Secondly, we test the weakest received signal from FAP_2 and FAP_3 which is −110 dB and −115 dB, respectively. Finally, the new transmission power for FAP_2 is 2 dB and for FAP_4 is 7 dB. FUE_4 receives a signal only from FAP_2 and FAP_4 is the only FAP that can provide the service for FUE_5 and FUE_6 as shown on Fig. 18 and reported on Table 18. Table 19 shows the difference between the hybrid approach and the proposed in [9], in case of these three FUEs. Our hybrid approach

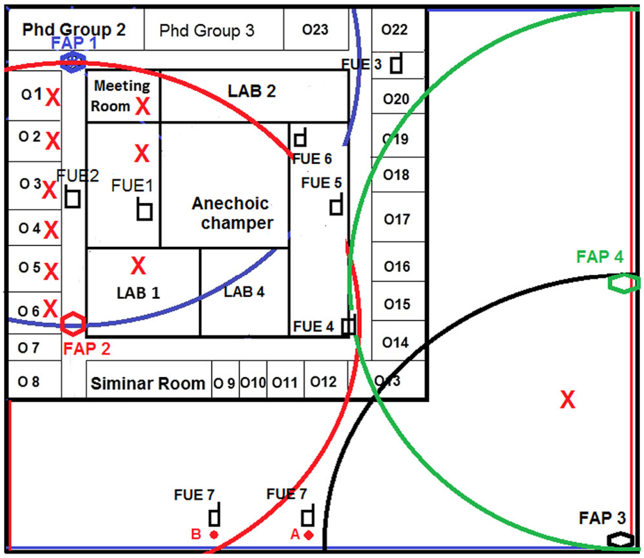

Fig. 49. FAPs and FUEs in relation to interference locations.

outperforms this study in terms of providing coverage, mitigating outage and increasing the number of FUEs. FUE_6 experiences no service at all and the rest of the FUEs receive very poor signals. The hybrid approach guarantees a service to all users that require the service.

The study presented in [29] proposes a new way to predict the required number of FAPs and their optimum location. It is suggested that FAPs are located with consideration of macrocell interference and the level of SINR for each FAP. The study aims at predicting the minimum number of FAPs that meets the coverage demand. The distance between FAP_1 and the macrocell and to the rest of the FAPs is set at 2 × a, where a is the half coverage radio. Moreover, the cell is formed in a hexagonal shape. The authors suggest deploying the first FAP close to the macrocell so we deploy FAP_1 in office 5 where it can provide higher coverage than the rest of the offices on the left. We deploy the rest of the FAPs at 60 m away from FAP_1 hexagonally. Fig. 40 shows that the area is covered but none of the FAPs can serve the left part of LAB2 due to the anechoic chamber absorbing the signal from FAP_1 and the high penetration loss that severely attenuates the signal from FAP_2. Fig. 41 shows deployment of the three FAPs with their radius coverage. This shows severe outages from FAP_2 and FAP_3 in LAB 3. This LAB suffers from lack of service from the macrocell and FUE_4, FUE_5, and FUE_6 are located in this LAB. Where FUE_4 is located, there is no received signal either from the macrocell or from the FAPs. Table 20 shows a comparison between our approach and this study in relation to FUE_4. Our approach outperforms the approach in [29] in terms of increasing coverage, reducing outage and battery drain.

The study presented in [30] suggests that any area is divided into sub-regions equally, where each sub-region is 4 m × 4 m and the FAPs are located where there is no potential interference from the macrocell nor other FAPs. Following that if an FUE receives a poor signal, the FUE increases its transmission power to meet the required service. Fig. 42 shows the deployment of femtocells inside the area.

The dimensions of the target area used in the study is 48 m × 48 m and it requires 5 FAPs to be installed due to the high penetration loss. The number of FAPs is high for this size as the potential of interference is high due to the close distance between FAPs. Moreover, the user uplink transmission power is controlled to avoid the interference by optimising SINR. This means that in the case of movement, transmission power is increased which may affect power consumption. Another disadvantage with this study, is that it does not predict the number of FAPs before deployment so the number of FAPs is only defined after the end of the deployment. With our approach, in consideration of the penetration loss and interference, the required number of FAPs is 4 regardless of the college being larger than the building used in the study of [30]. We start by dividing the area into 4 m × 4 m sub-regions and then clustering the sub-regions to deploy a FAP in each cluster. The cluster is based on coverage and low level of interference. Figs. 43 and 44 show how to cluster the area and deploy FAPs considering the coverage and interference. The hall is selected to install FAP_1 and FAP_2 is installed inside LAB3 where there is no interference from FAP_1 and the macrocell. The rest of FAPs are deployed outdoor as far as possible from one another to minimise the co-tier interference. Some of the target area experiences poor service due to the long distance from FAPs, e.g. LAB1. If FUE_2 moves to LAB1, it will receive two poor signals and as the best FAP cannot be predicted, FUE_2 will be connected randomly to one of these two FAPs. We compare the case of movement of FUE_2 using both the hybrid approach and the proposed study. Figs. 45 and 46 show the received power from both FAPs in case of the hybrid approach and the approach in [30]. FAP_2 is selected as the BN in our approach as it offers a high RSCP to FUE_2 but not with the approach of [30]. Table 21 shows the FUE_2 RSCP values from both FAPs using the hybrid approach and that in [30]. Our approach outperforms the approach in [30] in providing high power which enhances power consumption and manages interference by blocking a connection between FAP_1 and FUE_2.

In [31] an ushering method is proposed that provides users with optimum locations to avoid interference. This method also suggests best locations for browsing and using specific software applications. Fig. 47 shows the results after applying this method inside a 42 m × 42 m target area. We apply his method inside the college to show interference locations and the effectiveness of this algorithm in relation to the hybrid approach. Figs. 48 and 49 show the college after applying the ushering mechanism to identify interference locations. All users inside offices 1 through to 6, the corridor, meeting room, PhD room 1, LAB1 and the right lower hand corner are vulnerable to interference and will need to relocate to avoid interference. The hybrid approach outperforms the algorithms in terms of managing interference and without requiring users to move their FUEs.

7. Concluding discussion

The focus of this paper is managing both types of interference, co-tier and cross-tier, and improving the femtocell performance in terms of coverage, number of users and quality of its service. Moreover, our approach addresses the problem of dead zones and battery drain. A new hybrid technique based on transmission power calibration has been presented that can be applied to manage both types of interference. This technique identifies a BN either as the macrocell or a FAP deployed in the coverage area. A BN is identified by considering three factors: RSCP, multipath and, Distance. After finding the BN to an FUE, all other nodes are blocked from connecting to that FUE to prevent interference. An FUE keeps its connection to its BN, if the FUE is not receiving a signal from another node, to prevent the probability of an outage. The new deployment plan for femtocell technology can be applied in both environments: indoors and outdoors and our results suggest that operator networks can extend and maximise their number of users and in turn reduce the probability of outage. Our hybrid three-phase approach predictions are evaluated against the predictions of several models that have been reported in our literature review and it is shown that our approach outperforms these models. In relation to the three-phase approach, future R&D may include additional parameters such as network throughput to consider the effect on capacity during deployment and on spectral efficiency during power control. Throughput may be optimised by increasing the initial transmission power with consideration paid to the potential change in the transmission power value during the third phase. Additional parameters to include are building height during the first phase, and handset antenna gain during the third phase, with the latter of the two possibly helping to achieve a higher level of quality of service among users. Furthermore, incorporating clustering techniques in the three-phase approach to assign portions of the available spectrum to FAPs and macrocells may also be considered if the number of FAPs and macrocells is significantly high and allocation in dedicated channels may help with minimising both types of interference.

References

[1] K. Rajesh, What are femtocells and what are their advantages and disadvantages, 2009, [Online]. Available: http://www.excitingip.com/182/what-are-femtocells-and-what-are-their-advantages-and-disadvantages/.

[2] T. Zahir, K. Arshad, A. Nakata, K. Moessner, Interference management in femtocells, IEEE Commun. Surv. Tutor. 15 (1) (2013) 293–311.

[3] H. Kpojime, G. Safdar, Interference mitigation in cognitive radio based femtocells, IEEE Commun. Surv. Tutor. 17 (3) (2015) 1511–1534.

[4] V.U. Sankar, V. Sharma, Subchannel allocation and power control in femtocells to provide quality of service, in: 2012 National Conference on Communications (NCC), 2012.

[5] N. Saquib, E. Hossain, L.B. Le, D.I. Kim, Interference management in OFDMA Femtocell networks : issues and approaches, IEEE Wirel. Commun. (2012) 86–95.

[6] K. Rathan, Bandwidth allocation in wireless mesh network using efficient path selection scheme, Int. Rev. Comput. Softw. 10 (6) (2015).

[7] S.K.M. Bargavi, G.P. Rajamani, Energy consumption in wireless ad hoc network using ERCIM, Int. Rev. Comput. Softw. 9 (6) (2014) 831–835.

[8] S. Nagaraja, V. Khaitan, Y. Jiang, C. Patel, F. Meshkati, Y. Tokgoz, M. Yavuz, Downlink transmit power calibration for enterprise femtocells, IEEE Veh. Technol. Conf. (Dl) (2011) 0–4.

[9] K.C. Ting, H.C. Wang, C.C. Tseng, F.C. Kuo, H. Te Huang, Downlink co-tier interference mitigation for femtocell networks, in: 2014 Tenth Int. Conf. Intell. Inf. Hiding Multimed. Signal Process., 2014, pp. 898–901.

[10] J. Wang, L. Wang, Q. Wu, P. Yang, Y. Xu, J. Wang, Less is more : Creating spectrum reuse opportunities via power control for OFDMA femtocell networks, IEEE Syst. J. (2016) 1–12.

[11] C. Tseng, C. Peng, H. Wang, Co-tier uplink power control in femtocell networks by Stackelberg game with pricing *, in: 2014 4th International Conference on Wireless Communications, Vehicular Technology, Information Theory and Aerospace & Electronic Systems (VITAE), no. 102, 2014, pp. 3–7.

[12] J.E. Håkegård, A. Lie, T.A. Myrvoll, Power control in HetNets and cognitive networks, in: 2012 Int. Symp. Commun. Inf. Technol. Isc. 2012, 2012, pp. 568–573.

[13] F.H. Khan, Y.J. Choi, Towards introducing self-configurability in cognitive femto-cell networks, in: Annu. IEEE Commun. Soc. Conf. Sensor, Mesh Ad Hoc Commun. Networks Work, vol. 1, 2012, pp. 37–39.

[14] H. Saad, A. Mohamed, T. ElBatt, Distributed cooperative Q-learning for power allocation in cognitive femtocell networks, in: 2012 IEEE Veh. Technol. Conf. (VTC Fall), 2012, pp. 1–5.

[15] S.E. Nai, T.Q.S. Quek, Coexistence in two-tier femtocell networks: Cognition and optimization, in: 2012 Int. Conf. Comput. Netw. Commun. ICNC'12, 2012, pp. 655–659.

[16] K. Vadivukkarasi, R. Kumar, Enhancement of indoor localization by path-loss reduction using modified rssi technique, Int. Rev. Comput. Softw. 9 (5) (2014) 865–871.

[17] K. Vadivukkarasi, R. Kumar, A novel algorithm to improve indoor localization accuracy and path-loss reduction using real time RSSI, Int. Rev. Comput. Softw. 10 (3) (2015) 332–339.

[18] C. Patel, V. Khaitan, S. Nagaraja, F. Meshkati, Y. Tokgoz, M. Yavuz, Downlink interference management techniques for residential femtocells, in: IEEE Int. Symp. Pers. Indoor Mob. Radio Commun. PIMRC, 2011, pp. 117–121.

[19] S. Nagaraja, V. Chande, S. Goel, F. Meshkati, M. Yavuz, Transmit power self-calibration for residential UMTS/HSPA femtocells, in: 2011 Int. Symp. Model. Optim. Mobile, Ad Hoc, Wirel. Networks, WiOpt 2011, 2011, pp. 451–455.

[20] Z. Jako, G. Jeney, Coverage analysis of matérn cluster based LTE small cell networks, in: 2014 Eighth International Conference on Next Generation Mobile Apps, Services and Technologies, 2014, pp. 229–234.

[21] S.M. Asif, K.S. Kwak, Downlink coverage and rate analysis of two-tier networks, IEEE Wirel. Commun. Lett. 4 (2015) 133–136.

[22] M. M.Garcia, J.C. Sánchez, A.F. Durán, J.I. Alonso, Novel gentic algorithm for computer aided optimization of multi-femtocell deployments, in: 19th International Conference on Systems, Signals and Image Processing (IWSSIP), 2012, pp. 261–264.

[23] S.F. Yunas, A. Asp, J. Niemela, M. Valkama, Deployment strategies and performance analysis of Macrocell and Femtocell networks in suburban environment with modern buildings, in: Proc. - Conf. Local Comput. Networks, LCN, 2014–Novem, no. November, 2014, pp. 643–651.

[24] S.-E. Wei, C.-H. Chang, Y.-E. Lin, H.-Y. Hsieh, H.-J. Su, Formulating and solving the femtocell deployment problem in two-tier heterogeneous networks, in: IEEE Int. Conf. Commun., 2012, pp. 5053–5058.

[25] E.B. Rodrigues, F. Casadevall, Optimal distributed frequency planning for OFDMA femtocell networks, in: IEEE Int. Symp. Pers. Indoor Mob. Radio Commun. PIMRC, 2013, pp. 2914–2918.

[26] J. Liu, T. Kou, Q. Chen, H.D. Sherali, Femtocell base station deployment in commercial buildings: A global optimization approach, IEEE J. Sel. Areas Commun. 30 (3) (2012) 652–663.

[27] J. Jagadeesan, M. Riihijaarvi, Impact of three-dimensionality of femtocell deployments on aggregate interference estimation, in: IEEE Int. Symp. Pers. Indoor Mob. Radio Commun. PIMRC, 2015, pp. 737–742.

[28] L. Zhang, L. Yang, T. Yang, Cognitive interference management for LTE-A femtocells with distributed carrier selection, in: Vehicular Technology Conference Fall (VTC 2010-Fall), 2010 IEEE 72nd, 2010, pp. 1–5.

[29] M. Tahalani, V. Sathya, U.S. Suhas, R. Chaganti, B.R. Tamma, Optimal femto placement in enterprise building, Adv. Netw. Telecommun. Syst. (4) (2013) 4–6.

[30] A. Ramamurthy, V. Sathya, V. Venkatesh, R. Ramji, B.R. Tamma, Energy-efficient Femtocell placement in LTE networks, in: 2015 IEEE Int. Conf. Electron. Comput. Commun. Technol. 2015, pp. 1–6.

[31] C. Wang, S. Member, S. Fang, S. Member, H. Wu, Novel user-placement ushering mechanism to improve quality-of-service for femtocell networks, IEEE Syst. J. PP (99) (2017) 1–12.

[32] F. Zhao, H. Nie, H. Chen, Group buying spectrum auction algorithm for fractional frequency reuse cognitive cellular systems, Ad Hoc Netw. 58 (2017) 239–246.

[33] A.A. Alotaibi, M.C. Angelides, A hybrid approach for femtocell co-tier interference mitigation, in: 12th International Conference for Internet Technology and Secured Transactions, ICITST-2017, 2017.

[34] A. Gouissem, R. Hamila, N. Aldhahir, S. Foufou, Secondary users selection and sparse narrow-band interference mitigation in cognitive radio networks, Comput. Commun. 123 (February) (2018) 97–115.

[35] J. Yu, S. Han, X. Li, A robust game-based algorithm for downlink joint resource allocation in hierarchical OFDMA femtocell network system, IEEE Trans. Syst. Man, Cybern. Syst. (2018) 1–11.

[36] Y. Chen, X. Yin, Joint price competition and resource allocation for duopoly femtocell market, IEEE Trans. Veh. Technol. 67 (3) (2018) 2491–2500.

[37] C. Wang, W.H. Kuo, C.Y. Chu, QoS-aware cooperative power control and resource allocation scheme in LTE femtocell networks, Comput. Commun. 110 (2017) 164–174.

[38] A.S.M.Z. Shifat, M.Z. Chowdhury, Y.M. Jang, Game-based approach for QoS provisioning and interference management in heterogeneous networks, IEEE Access PP (99) (2017) 1–13.

[39] Y.L. Lee, J. Loo, T.C. Chuah, Dynamic resource management for LTE-based hybrid access femtocell systems, IEEE Syst. J. 12 (1) (2018) 959–970.

[40] J. Cao, T. Peng, Z. Qi, R. Duan, Y. Yuan, W. Wang, Interference management in ultra-dense networks: A user-centric coalition formation game approach, IEEE Trans. Veh. Technol. 9545 (c) (2018).

[41] Z. Liu, P. Zhang, X. Guan, H. Yang, Joint subchannel and power allocation in secure transmission design for femtocell networks, IEEE Syst. J. (2018) 1–11.

[42] Z. Liu, S. Li, K. Ma, X. Guan, X. Li, Robust power allocation based on hierarchical game with consideration of different user requirements in two-tier femtocell networks, Comput. Netw. 122 (2017) 179–190.

[43] S. Ghosh, V. Sathya, A. Ramamurthy, A. B, B.R. Tamma, A novel resource allocation and power control mechanism for hybrid access femtocells, Comput. Commun. 109 (2017) 53–75.

[44] S.A. Saad, M. Ismail, R. Nordin, A.U. Ahmed, A fractional path-loss compensation based power control technique for interference mitigation in LTE-A femtocell networks, Phys. Commun. 21 (2016) 1–9.

[45] P. Hu, J. Ye, F. Zhang, S. Deng, C. Wang, W. Wang, Downlink resource management based on cross- cognition and graph coloring in cognitive radio femtocell networks, in: 2012 IEEE Vehicular Technology Conference (VTC Fall), 2012.

[46] Y. Saleem, A. Bashir, E. Ahmed, J. Qadir, A. Baig, Spectrum-aware dynamic channel assignment in cognitive radio networks, in: 2012 International Conference on Emerging Technologies, 2012, pp. 1–6.

[47] S. Bose, B. Natarajan, Reliable spectrum sensing for resource allocation of cognitive radio based WiMAX femtocells, Consum. Commun. Netw. Conf. (CCNC), 2012 IEEE, 2012, pp. 889–893.

[48] L. Li, C. Xu, M. Tao, Resource allocation in open access OFDMA femtocell networks, IEEE Wirel. Commun. Lett. 1 (6) (2012) 625–628.

[49] Y. Ma, T. Lv, J. Zhang, H. Gao, Y. Lu, Cognitive interference mitigation in heterogeneous femto-macro cell networks, in: IEEE Int. Symp. Pers. Indoor Mob. Radio Commun. PIMRC, 2012, pp. 2131–2136.

[50] S.M. Cheng, W.C. Ao, F.M. Tseng, K.C. Chen, Design and analysis of downlink spectrum sharing in two-tier cognitive femto networks, IEEE Trans. Veh. Technol. 61 (5) (2012) 2194–2207.

[51] Y.S. Soh, T.Q.S. Quek, M. Kountouris, G. Caire, Cognitive hybrid division duplex for two-tier femtocell networks, IEEE Trans. Wirel. Commun. 12 (10) (2013) 4852–4865.

[52] S. Leveil, Le Martret, J. Christophe, H. Anouar, K. Arshad, T. Zahir, J. Bito, U. Celentano, G. Mange, J. Rico, A. Medela, Resource management of centrally controlled cognitive radio networks, Futur. Netw. Mob. Summit (2012) 1–9.

[53] E. Mugume, W. Prawatmuang, D.K.C. So, Cooperative spectrum sensing for green cognitive femtocell network, in: IEEE Int. Symp. Pers. Indoor Mob. Radio Commun. PIMRC, 2013, pp. 2368–2372.

[54] X.Y. Wang, P.-H. Ho, Kwang-Cheng Chen, Interference analysis and mitigation for cognitive-empowered femtocells through stochastic dual control, IEEE Trans. Wirel. Commun. 11 (6) (2012) 2065–2075.

[55] M. Li, S. Salinas, S. Member, P. Li, Optimal scheduling for multi-radio multi-channel multi-hop cognitive cellular networks, IEEE Trans. Mob. Comput. 14 (1) (2015) 139–154.

[56] Y. Du, M. Li, Y. Huang, X. Gao, S. Jin, Pilot scheduling schemes for multi-cell massive multiple-input–multiple-output transmission, IET Commun. 9 (5) (2015) 689–700.
[57] H. Zhang, C. Jiang, X. Mao, H.-H. Chen, Interference-limited resource optimization in cognitive femtocells with fairness and imperfect spectrum sensing, IEEE Trans. Veh. Technol. 9545 (c) (2015) 1–1.
[58] Y. Han, E. Ekici, H. Kremo, O. Altintas, Spectrum sharing methods for the coexistence of multiple RF systems: A survey, Ad Hoc Netw. 53 (2016) 53–78.
[59] M. Ahmed, J. Kim, Context aware network-assisted hand-off management and interference mitigation scheme for heterogeneous networks, in: Wireless Communications and Networking Conference (WCNC), vol. 3, 2013, pp. 3012–3017.
[60] A. Hatoum, R. Langar, N. Aitsaadi, R. Boutaba, G. Pujolle, Cluster-based resource management in OFDMA Femtocell networkswith QoS guarantees, Veh. Technol. IEEE Trans. 63 (5) (2014) 2378–2391.
[61] C. Bouras, G. Diles, V. Kokkinos, A. Papazois, Femtocells coordination in future hybrid access deployments, in: 2014 11th International Symposium on Wireless Communications Systems (ISWCS), 2014, pp. 313–317.
[62] B. Niu, V. Wong, Network configuration for two-tier macro-femto systems with hybrid access, IEEE Trans. Veh. Technol. 65 (4) (2016) 2528–2543.
[63] M.Z. Shakir, R. Atat, M.S. Alouini, On the interference suppression capabilities of cognitive enabled femto cellular networks, in: Int. Conf. Commun. Inf. Technol. - Proc. 2012, pp. 402–407.
[64] S. Salari, I. Kim, S. Member, D.I. Kim, S. Member, F. Chan, S. Member, Joint EH time allocation and distributed beamforming in interference-limited two-way networks with EH-based relays, IEEE Trans. Wirel. Commun. 16 (10) (2017) 6395–6408.
[65] F.A. Almalki, M.C. Angelides, Considering near space platforms to close the coverage gap in wireless communications; the case of the Kingdom of Saudi Arabia, in: FTC 2016 - Future Technologies Conference, 2016.
[66] A.U. Chaudhry, R.H.M. Hafez, J.W. Chinneck, Realistic interference-free channel assignment for dynamic wireless mesh networks using beamforming, Ad Hoc Netw. 51 (2016) 21–35.
[67] F.A. Almalki, M.C. Angelides, Empirical evolution of a propagation model for low altitude platforms, in: Computing Conference 2017, 2017.
[68] J. Garcá-Morales, G. Femenias, F. Riera-Palou, Statistical analysis and optimization of a 5th-percentile user rate constrained design for FFR/SFR-aided OFDMA-based cellular networks, IEEE Trans. Veh. Technol. PP (99) (2017) 1–14.
[69] A.R. Elsherif, W.-P. Chen, A.I. Ding, Adaptive resource allocation for interference management in small cell networks, IEEE Trans. Commun. 63 (6) (2015) 2107–2125.
[70] B. Xie, Z. Zhang, R.Q. Hu, G. Wu, A. Papathanassiou, Joint spectral efficiency and energy efficiency in FFR based wireless heterogeneous networks, IEEE Trans. Veh. Technol. 9545 (c) (2017) 1–14.
[71] W. Wang, F. Wang, Analytical evaluation of femtocell deployment in cellular networks using fractional frequency reuse, IET Commun. 8 (9) (2014) 1599–1608.
[72] G. Huang, J. li, Interference mitigation for femtocell networks via adaptive frequency reuse, IEEE Trans. Veh. Technol. (2016).
[73] J.H. Lim, R. Badlishah, M. Jusoh, LTE- Fractional Frequency Reuse (FFR) optimization with femtocell network, in: Electronic Design (ICED), 2014 2nd International Conference, 2014.
[74] A. Mahmud, K.A. Hamdi, On the co-channel femtocells exclusion region in fractional frequency reuse macrocells, in: Wireless Communications and Networking Conference (WCNC), 2014 IEEE, 2014.
[75] T.I. Giovany, U.K. Usman, B. Prasetya, Simulation and analysis of interference avoidance using fractional frequency reuse (FFR) method in LTE femtocell, in: 2013 International Conference of Information and Communication Technology (ICoICT), 2013.
[76] M. Rosdi, A.L. Yusof, M.T. Ali, N. Ya, M. Ismail, M.A. Zainali, M.S. Nasroali, B.A. Bakar, Capacity improvement for heterogeneous LTE network by using fractional frequency reuse method, 2014, pp. 37–42.
[77] J. Zhang, F. Jin, R. Zhang, G. Li, L. Hanzo, Analysis and design of distributed antenna-aided twin-layer femto-and macrocell networks relying on fractional frequency reuse, IEEE Trans. Veh. Technol. 63 (2) (2014) 763–774.
[78] A.A. Alotaibi, M.C. Angelides, Wireless femtocell coverage on the go: A case in the Kingdom of Saudi Arabia, in: IEEE UEMCON 2016-The 7th IEEE Annual Ubiquitous Computing, Electronics & Mobile Communication Conference, 2016.
[79] C. Campolo, C. Sommer, F. Dressler, A. Molinaro, On the impact of adjacent channel interference in multi-channel VANETs, in: IEEE ICC 2016 Ad-hoc and Sensor Networking Symposium, 2016.
[80] J. Yoon, M.Y. Arslan, K. Sundaresan, Characterization of interference in OFDMA small-cell networks, XX (XX) (2018) 1–17.
[81] A.A. Alotaibi, M.C. Angelides, Femtocell deployment plan : Moving indoors, in: Intelligent System Conference 2017, 2017.
[82] J. Dai, S. Wang, Clustering-based interference management in densely deployed femtocell networks, Digit. Commun. Netw. (2016) 175–183.
[83] A. Khalifah, N. Akkari, G. Aldabbagh, N. Dimitriou, Hybrid femto/macro rate-based offloading for high user density networks, Comput. Netw. 108 (2016) 371–380.
[84] X. Tao, Z. Zhao, R. Li, J. Palicot, H. Zhang, Downlink interference minimization in cognitive LTE-femtocell networks, in: 2013 IEEE/CIC Int. Conf. Commun. China, ICCC 2013, no. Iccc, 2013, pp. 124–129.
[85] H. Shi, E. Osman, Y. Hepsaydir and J., in: Wang Indoor Wirel. Femtocell Meas. IEEE ICC Wirel. Commun. Symp. London, 2015.